Integrated and agent-based charging demand prediction considering cost aware and adaptive charging behavior

Transportation Research Part D 154 (2026) 105285

Contents lists available at ScienceDirect

Transportation Research Part D

journal homepage: www.elsevier.com/locate/trd

Integrated and agent-based charging demand prediction considering cost aware and adaptive charging behavior

Omkar Parishwad [a], Kun Gao [a,*], Arsalan Najafi [a,b]

[a] Department of Architecture and Civil Engineering, Chalmers University of Technology, SE-412 96, Gothenburg, Sweden
[b] Department of Electrical Engineering Fundamentals, Wroclaw University of Science and Technology, 50-370, Wroclaw, Poland

ARTICLE INFO

Keywords:
Electromobility
Agent based modeling
MATSim
Future charging demand
Dynamic pricing
Charging behavior

ABSTRACT

With the projected growth of electric vehicles to meet net-zero emission targets, the accurate prediction of future charging demand is essential for optimal infrastructure planning. This study delivers an integrated and scalable agent-based modeling framework for future spatiotemporal estimation, which simultaneously captures heterogeneous cost aware charging behaviors, daily activity patterns, and route and mode choices. Meanwhile, the framework employs a stochastic, adaptive smart charging module that incorporates diverse charger types and dynamic ToU electric tariffs, enabling users to probabilistically shift charging decisions to minimize costs and mitigate range anxiety. The framework was applied in a case study of Gothenburg, Sweden, under near-future scenarios with 50 % EV penetration. Results indicate that introducing charger-type prices with residential ToU tariffs shifts charging toward home, and probabilistic ToU-aware deferral reduces the residential peak by upto 20 % relative to the cost aware but immediate charging scenario.

1. Introduction

The rapid adoption of electric vehicles (EVs) marks a transformative shift toward sustainable urban mobility driven by national and regional policy objectives to decarbonize the transport sector and meet net-zero emission targets (Rodrigues et al., 2023). EV integration can substantially reduce greenhouse gas emissions, improve urban air quality, and mitigate the environmental impact of transport systems (Muratori et al., 2021a). At the same time, with global EV penetration projected to be roughly 40 % of new vehicle sales by 2030, EVs alone may account for over 8 % of global electricity demand by 2035, implying non-trivial impacts on charging infrastructure needs and electricity grids (International Energy Agency, 2023; Rietmann et al., 2020). This creates an urgent need for modeling frameworks that can reliably estimate spatiotemporal future charging demand to support infrastructure deployment, grid management, and policy design (Kim and Kim, 2021).

Accurately estimating the future charging demand is challenging because EV charging behavior is inherently heterogeneous and context-dependent. The daily travel patterns differ across users and days, charging opportunities arise at multiple locations (home, workplace, public chargers), and vehicle types and battery capacities vary (Kamana-Williams et al., 2024; Li et al., 2024). Charging behavior is further shaped by external drivers, such as time of use (ToU) electricity pricing, smart charging technology, and charger access, which jointly influence when, where, and how users choose to charge to minimize perceived costs while maintaining a sufficient state of charge (SoC) for upcoming trips (Shariatzadeh et al., 2025; Thorhauge et al., 2024). These interacting factors give rise to highly spatiotemporal and activity-dependent charging patterns that cannot be captured by static or purely aggregate models.

* Corresponding author.
E-mail addresses: omkarp@chalmers.se (O. Parishwad), gkun@chalmers.se (K. Gao), arsalan.najafi@chalmers.se (A. Najafi).

https://doi.org/10.1016/j.trd.2026.105285
Received 16 August 2025; Received in revised form 30 December 2025; Accepted 13 February 2026
Available online 20 February 2026

Despite substantial advances in charging demand modeling, significant gaps remain. Many existing approaches rely on static or overly simplified assumptions that do not adequately represent the dynamic and probabilistic nature of user behavior under realistic spatiotemporal pricing and smart charging conditions (Yi et al., 2023; Wu et al., 2023b). Sensitivity to spatially and temporally variable electricity pricing is known to substantially affect charging timing and location choice (Visaria et al., 2022; Ensslen et al., 2018; He et al., 2025). However, large-scale agent-based simulations often still treat dynamic tariffs as exogenous signals or apply charging rules in post-processing, rather than embedding price response directly within the same utility-based scoring and iterative learning mechanism that governs travel choices and charging decisions (Liao et al., 2023). Moreover, even when ToU effects are represented, plug-in time is frequently conflated with charging start time and heterogeneous compliance with deferral is rarely modeled explicitly, such that only a subset of users reschedules feasible home sessions. This limits the credibility of spatiotemporal peak estimates under ToU considerations, and location specific charging opportunities are only partially captured (He et al., 2022; Kim and Kim, 2021). These limitations hinder the realistic emulation of individual charging patterns and reduce the reliability of spatiotemporal charging demand estimates for future scenarios, thereby constraining the usefulness of such models for infrastructure and energy side infrastructure planning and management.

To address the aforementioned gaps, this study proposes an integrated modeling and analytical framework based on agent-based modeling to estimate the future spatiotemporal EV charging demand. The framework captures EV users' charging decisions by incorporating their daily travel behavior (including activity chains, mode and route choices) and charging behavior, which seeks to minimize costs under ToU electricity pricing. Meanwhile, it accounts for heterogeneous charging costs across different charging types and incorporates smart charging strategies. A key contribution of this study is the development of a probabilistic and adaptive smart charging module that allows users to reschedule charging events within the plugged-in time window to make the most of ToU electricity price variations. This module is embedded in an extended scoring function in MATSim that jointly models mode choice, route choice, and charging behavior, thereby capturing realistic user trade-offs that are often neglected in existing models. To the best of our knowledge, this study is among the early large-scale agent-based implementations that embed charger type monetary costs and ToU-aware intra activity start-time rescheduling directly into the EV behavioral scoring, building on prior MATSim pricing frameworks that decouple plug-in and charging times for tariff experiments (Bakhtiari et al., 2024, 2023). Unlike rule based or threshold-driven approaches, the proposed framework adopts a holistic and utility-optimization based modeling strategy that yields a behaviorally consistent representation of user charging decisions over a continuous, multi-day horizon that captures weekly charging routines rather than isolated single-day decisions. Applied to a near-future scenario with 50 % EV penetration in Gothenburg, Sweden, the model reveals how spatiotemporal variations in charging costs and the adoption of smart charging significantly influence individual charging decisions, ultimately shaping aggregated spatiotemporal charging demand patterns. The scalability and adaptability of the approach ensure its applicability across diverse urban contexts. The results offer a scientific foundation for estimating future charging demand and informing the cost-efficient planning of charging infrastructure and energy systems to support transport electrification.

The remaining parts of this paper are structured as follows. Section 2 reviews prior work on EV charging demand modeling and agent-based approaches. Section 3 describes the proposed modeling framework, including the inherited UrbanEV utility terms and the new cost aware and ToU aware extensions. Section 4 presents the Gothenburg case study, input data, and parameterization. Section 5 reports the temporal and spatial charging demand results across scenarios. Finally, Section 6 concludes with implications, limitations and outlines directions for future research.

2. Literature review

Before introducing our integrated modeling framework, we review existing approaches to EV charging demand estimation, highlighting their strengths and limitations. Beginning with foundational studies to estimate hourly EV energy demand, we scope the evolution from static and rule based models to enhanced agent-based frameworks, to justify the critical research gaps that motivated our work.

2.1. Aggregated demand estimation models

Traditional approaches to EV charging demand estimation have predominantly utilized static models, such as origin-destination matrices and rule based frameworks. Dharmakeerthi et al. (2014) employed a static model with fixed state of charge (SoC) thresholds, assuming homogeneous charging behavior among users. Similarly, Deb et al. (2018) noted that while these models offer computational efficiency, they often lead to significant discrepancies when applied to heterogeneous urban environments characterized by diverse daily travel patterns and varying charger availability. These methods typically treat charging demand as a static variable, overlooking the dynamic and stochastic nature of user behaviors, temporal variability, and spatial heterogeneity. Shukla et al. (2023) optimized EV charger placement using a static OD matrix but acknowledged its limitations in representing real-time spatiotemporal demand. Likewise, Celik (2024) reviewed deterministic models and highlighted their inability to adapt to evolving user preferences and grid constraints, thereby limiting their utility in dynamic scenarios.

To address the limitations of static models, dynamic models have been developed to incorporate temporal variations in charging demand. Tan et al. (2022) proposed a dynamic pricing strategy based on traffic assignment simulation, wherein charging prices are updated according to the temporal distribution of EV charging demand. Such approaches often use differential equations or simulation based methods to model the system's temporal response under varying price conditions. However, despite their improved responsiveness, these models largely depend on aggregated data and deterministic assumptions, smoothing over the nuances of individual charging behaviors, such as variations in range anxiety or the diversity of daily travel patterns. Consequently, they struggle

to capture the probabilistic and behaviorally heterogeneous nature of individual charging decisions, especially under conditions such as range anxiety and fluctuating daily trip patterns (Schüßler et al., 2017; Patil et al., 2023). These limitations are especially consequential under high EV penetration and tariff interventions, where charging is shaped by user specific charging tolerance and timing preferences. Consequently, demand estimation frameworks that remain aggregated or deterministic tend to under represent both the dispersion of charging start times and the partial, heterogeneous nature of price response.

2.2. Heterogeneous charging preferences and timing choice

A growing body of empirical and modeling research has emphasized that EV charging behavior is highly heterogeneous, both across users and across contexts, and cannot be captured adequately by homogeneous or purely deterministic charging rules. Wu et al. (2023a) propose a heterogeneous aggregation and control model for EV clusters with random charging behaviors, in which individual vehicles differ in battery parameters, charging power, and plug-in, plug-out times. Their work shows that aggregate controllability of EV fleets arises from underlying stochastic, heterogeneous individual actions rather than uniform optimization, and that realistic aggregation models must explicitly account for random charging start times and user-specific behavior. This supports treating charging as a stochastic, heterogeneous process and motivates the representation of probabilistic charging responses in demand models.

Building on an activity based perspective, Rostami et al. (2024) integrate travel demand, charging behavior, and charging infrastructure planning under alternative electricity tariff schemes. Using an activity based simulation for the Chicago region, they demonstrate that tariff structure strongly influences the spatial and temporal distribution of charging demand and, consequently, the optimal placement and sizing of fast-charging infrastructure. Their framework highlights that electricity pricing cannot be treated as exogenous when planning public charging networks. However, the focus remains on tariff-induced shifts in aggregated charging demand and infrastructure siting, rather than on individual-level, multi-criteria charging decisions embedded in a co-evolutionary day-to-day learning process. Micro-level choice experiments further clarify the determinants of individual charging decisions. Ge and MacKenzie (2022) analyze BEV drivers' fast-charging choices on long-distance trips using static and dynamic discrete choice models. They find that battery SoC and the ability to reach the next station without deviating from the planned route are the dominant determinants of charging, while charging cost, time, and detour length play secondary roles, consistent with recent syntheses on range anxiety and mid-trip charging behavior (Thorhauge et al., 2024; Wang et al., 2023). This confirms the primacy of state of charge and range-critical conditions in charging decisions and justifies the explicit modeling of range anxiety and SoC related penalties in behaviorally grounded charging frameworks. Complementary panel-data evidence from Japan by Sun et al. (2015) on home based charge timing shows that SoC at arrival, the number of days until the next travel day, and daily vehicle-kilometers traveled are key predictors of whether users charge immediately upon arrival, postpone charging to midnight, or do not charge at all. A substantial fraction of users adopt off-peak charging patterns, but many still charge immediately, indicating heterogeneity in both timing preferences and sensitivity to price or habitual considerations. These studies indicate that realistic charging demand models must represent SoC and range-driven risk aversion, heterogeneous and only partially price-responsive timing choices, and activity-dependent charging opportunities across home, work, and public contexts.

2.3. Probabilistic agent-based frameworks

Comparative evidence indicates that machine learning models can outperform conventional spatial interaction formulations when reproducing observed urban transport patterns (Parishwad et al., 2023). However, predictive accuracy alone is insufficient for our application, as charging demand under infrastructure and tariff interventions depends on behavioral adaptation, feasibility constraints, and schedule dependent decision making. For such counterfactual analyses, probabilistic random utility (logit based) choice mechanisms embedded in agent-based simulation provide an explicit behavioral mechanism through which prices, accessibility, and activity schedules translate into charging decisions.

Accordingly, recent advancements have increasingly leveraged agent-based modeling (ABM) to capture the complex and micro-level interactions inherent in EV charging behavior. Studies have demonstrated MATSim's ability to generate high-resolution hourly transport charging demand trends and to provide dynamic agent behaviors and travel patterns within energy system analysis, as examined by Novosel et al. (2015), who coupled MATSim outputs with their EnergyPLAN model. However, their work was limited by a narrow representation of daily activity chains (only home and work) and by its lack of explicit modeling of charging infrastructure, dynamic pricing, and diverse charging strategies. Building on this foundation, Zhuge and Shao (2018) extended MATSim by incorporating both link based and node based facility modeling, providing valuable insights into how the spatial distribution of charging facilities might influence user choices. Yet, the model oversimplified the charging decision process by assuming that EVs would charge at any available charging facility, without accounting for critical factors such as SoC, pricing, or variations in charger availability. More recently, Yi et al. (2023) employed MATSim to estimate public charging demand at an urban scale and optimized charging station locations via a capacitated maximal coverage approach. Their framework benefited from high-resolution synthetic demand validation against real-world records and considered different charger types, including both fast and standard. Despite these strengths, the model primarily focused on public charging and did not integrate the interplay between home and public charging, nor did it address the effects of dynamic pricing and spatiotemporal charging costs on user charging behavior. Complementing urban studies, Wu et al. (2023b) applied MATSim in a highway context to optimize EV charging infrastructure, modeling detailed decision processes, including charging station selection based on SoC, proximity, and travel time, suitable for long-haul travel scenarios. However, the study did not incorporate dynamic pricing or capture the full range of urban mobility patterns, thereby limiting its applicability to mixed-use environments.

In a further evolution, Adenaw and Lienkamp (2021) introduced UrbanEV, a co-evolutionary MATSim extension in which charging emerges from a utility based, multi criteria decision process rather than fixed SoC triggers. Building on the legacy EV Contrib energy and charger representation (ETH Zürich et al., 2016), UrbanEV augments plan scoring with battery-risk and access-friction components, using a range anxiety penalty for low SoC, a walking disutility term for access to off-route chargers, a strong penalty for empty-battery states, and a home-charging preference term incentivizing overnight charging at home. This co-evolutionary approach enables agents to adapt activity execution and route choice (Adenaw and Lienkamp, 2021). However, UrbanEV in its original form does not endogenize time varying electricity prices within the same scoring and learning mechanism, motivating extensions toward heterogeneous, tariff responsive timing adaptation. Several recent studies further demonstrate how UrbanEV and related EV Contrib developments have been applied, thereby documenting UrbanEV's role as a reusable behavioral backbone for urban electromobility analysis. Qiang et al. (2025) employ a MATSim based multi-agent trip simulation combined with an energy consumption model and charging rules to forecast spatiotemporal public charging demand in Japan. Their framework generates high-resolution daily trips and aggregates charging demand bottom-up, but charging decisions remain largely rule based, without explicit dynamic pricing or intra-activity rescheduling. Brulin et al. (2025) adapt the UrbanEV module to compare stationary charging infrastructure with battery-swapping concepts, using UrbanEV's activity based representation and SoC driven logic to evaluate detours, dwell times, and utilization in an urban network. These applications emphasize that UrbanEV's multi-criteria charging behavior has already been adopted beyond the original Munich case study, yet they still treat electricity prices exogenously and do not incorporate heterogeneous, tariff-responsive adaptations of charging timing.

A complementary line of work has focused more directly on pricing within MATSim. Bakhtiari et al. (2023) developed an EV charging pricing design framework that couples the legacy EV Contrib with an UrbanEV evolved within-day replanning procedure. They implement time-dependent, zonal, and nonlinear pricing schemes, demonstrating how different tariff designs can reduce peaks and redistribute charging temporally and spatially. Nevertheless, their implementation primarily targets public charging and operator-centric pricing scenarios, with charging strategies still driven by relatively stylized heuristics and with limited differentiation between home, work, and public charging contexts. In parallel, recent EV Contrib (MATSim v.2025) release (MATSim Community, 2025) emphasizes station-level realism with representations of individual charging behavior, including nonlinear charging curves, plug capacities, and queuing at individual stations, as demonstrated in neighborhood-scale applications such as the Das Neue Gartenfeld case study in Berlin (Kreuschner and Schlenther, 2025; Hörl et al., 2025). The latest EV Contrib capabilities are well suited to analyze current, station-level infrastructure utilization under specific operator pricing schemes and binding capacity constraints. For the present study, which assumes abundant charging capacity and seeks to reveal latent, near-future charging demand emerging from heterogeneous, multi-criteria, and price aware behavior, UrbanEV's co-evolutionary utility based framework provides a more appropriate behavioral backbone.

Other studies (Muratori et al., 2021b; Menter et al., 2023) have emphasized the potential of MATSim for large scale energy-mobility analyses, demonstrating the importance of high resolution travel data and the integration of network effects into infrastructure planning. Nonetheless, they also highlighted limitations in accounting for dynamic pricing and the interdependencies between varied daily activity chains and charging decisions. Finally, the literature (Parishwad et al., 2025b; Lin et al., 2024) provided a comprehensive technical review of EV charging distribution models, emphasizing the influence of driver behaviors on charging demand. Although their review laid a solid theoretical foundation, it did not fully integrate advanced ABM frameworks, such as MATSim, including dynamic pricing and smart charging considerations, which are crucial for understanding spatiotemporal demand fluctuations in urban contexts. While behavioral archetypes such as "plan-ahead" and "event-triggered" charging strategies have been identified in the literature, their integration into simulation models remains inadequate. Wongsunopparat and Cherian (2023) explored factors influencing consumer adoption of EVs but did not evaluate the implications of specific charging behaviors on infrastructure deployment. Similarly, Hartvigsson et al. (2022) conducted a geographic analysis of power system violations due to EV charging but did not incorporate diverse charging strategies into their modeling framework.

Building on these empirical and modeling insights into heterogeneous charging preferences and timing choice, UrbanEV offers a natural behavioral backbone. It already incorporates SoC driven risk, walking disutility, empty battery penalties, and home charging preferences in a co-evolutionary and plan based framework (Adenaw and Lienkamp, 2021). In this study, we evolve this framework by introducing additional utility components for charger type monetary costs at home, work, and public locations, monetary price sensitivity parameters that link charging expenditures to the underlying value of time and money, and ToU-aware rescheduling parameters, including stochastic awareness and coincidence factors that govern whether and how strongly agents shift charging within activity windows. Accordingly, the present study extends UrbanEV's co-evolutionary charging behavior with explicit cost awareness and probabilistic, ToU-aware intra-activity rescheduling to enhance spatiotemporal charging demand estimation under tariff interventions.

3. Methods

The EV charging demand estimation embedded within the MATSim framework extends the EV Contrib architecture (ETH Zürich et al., 2016) by integrating customized utility scoring extensions, elaborated in this section. Specifically, we adopt the UrbanEV extension of the original MATSim EV Contrib as the behavioral backbone for EV users (Adenaw and Lienkamp, 2021). This work extends it with the charger type specific monetary costs and ToU aware, home charging rescheduling, while MATSim's scoring and replanning loop handles activity execution, mode and route choice, and iterative learning under the same utility framework (Berlin, 2016). Each agent is assigned a daily activity plan that specifies a sequence of activities such as home, work, school, shopping, and associated travel legs. During simulation, agents execute these plans while performing SoC aware travel, charger compatibility

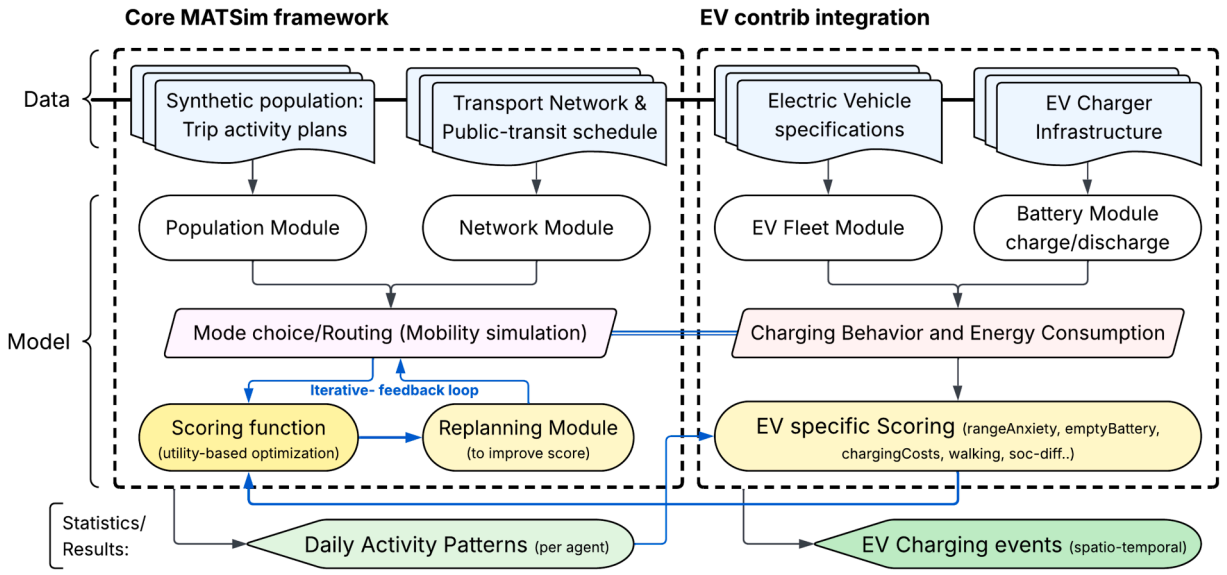

Fig. 1. MATSim integrated workflow for EV charging demand estimation.

checks, and dynamic insertion or rescheduling of charging events. A scoring mechanism based on utility functions that balances activity participation, travel time, and monetary cost guides iterative plan optimization (Arabani et al., 2024).

Fig. 1 illustrates the integrated framework we propose, wherein synthetic population activity plans, network topology, vehicle attributes, and charger infrastructure interact through iterative cycles of mobility simulation, EV specific scoring, and replanning. Charging events are dynamically inserted or scheduled in response to evolving SoC and behavioral triggers, with charger-EV compatibility enforced throughout the simulation. The conditional triggers illustrated in Fig. 1 should therefore be interpreted as an internal heuristic representation of a utility based decision process rather than as externally imposed rules. At every potential charging opportunity, agents evaluate the full EV specific utility described in Section 3.3: in low SoC states, range anxiety and empty battery penalties dominate and drive immediate charging, whereas deferral of home charging within an activity window is only considered when SoC is comfortably above the anxiety threshold and sufficient dwell time is available. Moreover, only a ToU aware subpopulation with imperfect compliance, governed by the awareness and coincidence factors introduced in Section 3.5, is eligible for such optimization. As a result, the model endogenously produces a spectrum of behaviors ranging from purely myopic to partially price responsive charging, rather than enforcing a single *intelligent* schedule for all EV users.

3.1. MATSim base framework and EV module integration

The deployed ABM enables an EV user behavior-centric representation for every agent, providing a detailed description of battery dynamics, energy consumption, interaction with charging infrastructure, and charging decisions. UrbanEV augments the MATSim plan score with EV specific utilities (range anxiety, empty battery penalties, and walking disutility), such that charging is adapted jointly with executed plans rather than imposed by fixed SoC triggers (Adenaw and Lienkamp, 2021). We retain this co-evolutionary structure and extend it with charger type monetary costs and residential ToU multipliers, enabling cost sensitive charging considerations and for home charging, start-time rescheduling within the plug-in window.

Agents may follow either an immediate charging (event-triggered) strategy, initiated when the SoC drops below a critical threshold and an urgent charging activity is needed, or a delayed (plan ahead) strategy, which defers charging during long-duration stops when SoC is sufficiently high. In the latter case, agents can reduce expected charging costs by selecting the charging location (and thus charger type), charging time, and charging start within the activity window. Start time selection is conducted via a utility maximizing search over feasible start times within the scheduled activity duration. If the required charging time exceeds the available idle time, agents initiate charging immediately at the onset of the activity, reverting to an event-triggered strategy. Chargers are characterized by their location, plug type, access classification (home, work, or public), outlet count, power rating, and charging cost parameters. For a given charging decision, the handler module selects a feasible charger by searching within a maximum walking radius around the activity location and applying UrbanEV's distance based and SoC based heuristics. Among compatible chargers inside the search radius, closer options are preferred unless SoC is critically low, in which case the nearest feasible charger is selected to avoid depletion. In line with the abundant-capacity assumption in this study, queuing and explicit waiting times at individual chargers are not modeled. Instead, plugs are assumed to be available whenever a compatible charger is selected, and the main behavioral trade-offs are captured through walking disutility, travel time impacts of detours, and monetary cost differences between charger types.

For home chargers, the charging price follows a time varying ToU electricity tariff derived from the power grid (Section 4). For workplace and public chargers, the charging price follows fixed per kWh rates provided by charging station operators or scenario

assumptions. Vehicles are characterized by attributes including battery capacity, SoC, energy consumption rate, and compatible plug profile. These components are integrated into the overall plan utility, enabling agents to trade off cost and utility during replanning. This intra-activity optimization constitutes the core of the adaptive smart charging construct introduced in this paper and is formalized in the subsequent subsections via the extended EV scoring formulation and the ToU aware rescheduling algorithm. Within each iteration, agents execute travel and charging events, and plan scores are updated to reflect utility changes induced by charging decisions based on the extended scoring formulation. A `BestScore` mutator, augmented with EV specific scoring, is employed for replanning, enabling the joint optimization of travel and charging schedules while converging toward a stable travel–charging pattern for all agents. The integrated framework enables the consideration of adaptive smart charging under varying tariff structures and infrastructure scenarios. System level outcomes, such as spatiotemporal demand profiles, peak load shifts, and charger utilization, are generated endogenously from individual charging profiles (when, where, and how each EV is charged). It is worth noting that the described strategies are moderated by two stochastic, configurable parameters: the awareness factor, which denotes the fraction of agents that respond to pricing signals, and the coincidence factor, which represents the likelihood that agents ignore cost-optimal start times when making charging decisions. Together, these parameters model user heterogeneity in charging behavior preferences. The following subsections first summarize the EV specific utility components inherited from UrbanEV and then detail the additional cost aware and ToU aware scoring and rescheduling mechanisms introduced in this study, which together define the cost sensitive adaptive smart charging behavior analyzed in the results.

3.2. Data integration and agent attribute specification

In the modeling, we consider each user's daily activity chains, which are important determinants of EV users' charging patterns. We integrate a synthetic population of agents. Each agent represents a human and has a daily activity chain and socio-demographic attributes. For each agent, a daily activity sequence consists of primary activities (home, work, public), mode choice, and route choice connecting two sequential activities. These plans were generated from empirical distributions of activity types, start times, durations, modes, and spatial origins and destinations using validated methodologies. More details about the synthetic population data used are available in the research by Tozluoglu et al. (2023).

For vehicles in the modeling framework, we consider different types of vehicles that imitate reality. Each EV is assigned specific attributes, including a specific EV model class, battery capacity, energy consumption rate, charger access type, and eligibility for adaptive smart charging. These attributes were encoded using the person (agent) and vehicle XML schema of the MATSim framework, and instantiated through the e-vehicles and population configuration files. Vehicle energy consumption and battery properties govern the evolution of SoC during trips and constrain eligibility for charging events at specific charger nodes (Liu et al., 2024). The road network was imported from cleaned OpenStreetMap data and converted into an attributed MATSim-compatible XML format, retaining geospatial accuracy, eligibility for specific modes, link capacities, functional hierarchy, and speed attributes. EV charging infrastructure was modeled using an additional XML input file that contained charger nodes with defined coordinates, plug types, access classifications, outlet counts, and power ratings. Agents without explicit private charger assignment (home and workplace) are probabilistically attributed to chargers using scenario specific penetration rates and proximity based assignment radius (Section 4). All spatial layers, including the road network, agent origins/destinations, and charger nodes, were projected to a common coordinate system. This enables distance and accessibility calculations that are internally consistent across inputs. Travel times, energy depletion, and walking disutilities were derived using network link attributes in combination with agent and vehicle characteristics. Time-dependent electricity prices were represented through a dimensionless ToU multiplier $M_{\mathrm{ToU}}(t)$, reflecting hourly residential ToU tariffs. During population initialization, each agent is assigned a binary person attribute `smartChargingAware` with probability f_{aware} (see Section 4.6). Only this subgroup accesses $M_{\mathrm{ToU}}(t)$ in real time and incorporates ToU varying costs into home charging decisions. As a result, charging demand emerged endogenously whenever trip based energy depletion intersected with charger availability, activity duration, electricity price information, and individual decision parameters.

Lastly, various studies such as Llorca and Moeckel (2019), which replicate simulations with different random seeds, verify a low variance in plan scores and network performance indicators. The adopted 10 % sampling rate is therefore consistent with established MATSim sampling-fidelity analyses (Kuehnel et al., 2022), while avoiding the high computational cost of explicitly simulating the full population.

3.3. Inherited utility parameters modeling charging behavior

Agent decision-making is incorporated as a discrete choice process within MATSim's co-evolutionary scoring functionality (Berlin, 2016), where the daily plans of multiple agents are iteratively scored and selected probabilistically based on a pseudo-random and utility maximization algorithm. In this study, the EV specific part of the scoring function inherits the co-evolutionary charging behavior introduced by the UrbanEV framework (Adenaw and Lienkamp, 2021), and incorporates its utility components through the standard MATSim scoring functionality. The agents iteratively select and mutate plans to improve their own score. This optimization enables the simulation to reflect real-world decision dynamics. The total plan score, S^{*}_{plan}, aggregates activity utilities and travel disutilities across all N segments.

$$S^{*}_{\mathrm{plan}} = \sum_{q=0}^{N-1} S_{\mathrm{act},q} + \sum_{q=0}^{N-1} S_{\mathrm{trav},q}, \tag{1}$$

where activity utility, $S_{\text{act},q}$ is specified as,

$$S_{\text{act},q} = \beta_{\text{dur}} \ln\left(\frac{t_{\text{dur},q}}{t_{\text{dur},0}}\right) + \beta_{\text{early}}\, t_{\text{early},q} + \beta_{\text{late}}\, t_{\text{late},q}. \tag{2}$$

Here, β_{dur} is the marginal utility of activity duration, $t_{\text{dur},0}$ is a normalization constant, and $\beta_{\text{early}}, \beta_{\text{late}}$ are penalties for schedule deviation. While the travel disutility, $S_{\text{trav},q}$, encompasses mode-specific costs (C), travel-time penalties, distance costs, monetary expenditures, and transfer penalties as defined here, in Eq. (3).

$$\begin{aligned} S_{\text{trav},q} = {} & C_{\text{mode}(q)} + \beta_{\text{trav,mode}(q)}\, t_{\text{trav},q} + \beta_m\, \Delta m_q \\ & + \left(\beta_{d,\text{mode}(q)} + \beta_m \gamma_{d,\text{mode}(q)}\right) d_{\text{trav},q} + \beta_{\text{transfer}}\, x_{\text{transfer},q}. \end{aligned} \tag{3}$$

Beyond the generic MATSim activity and travel terms in Eqs. (2) and (3), UrbanEV augments the plan score with EV specific components that capture battery related constraints and charging behavior. As formulated by Adenaw and Lienkamp (2021), these components include a range anxiety penalty for low SoC levels, an empty-battery penalty, and a walking disutility for off-route chargers, which are evaluated along each agent's executed plan and added to the standard plan utility. For EV agents, the EV augmented plan scoring function is defined as follows.

$$\begin{aligned} S_{\text{EV,plan},a} = {} & S^{*}_{\text{plan},a} + \beta_{\text{homeCharging}}\, S_{\text{homeCharging},a} + \beta_{\text{rangeAnxiety}}\, S_{\text{rangeAnxiety},a} \\ & + \beta_{\text{emptyBattery}}\, S_{\text{emptyBattery},a} + \beta_{\text{walk}}\, S_{\text{walking},a} + \beta_{\text{SoCdiff}}\, S_{\text{SoCdiff},a} \\ & + \alpha_{\text{scaleCost}}\, \beta_{\text{money}}\, C_{\text{ch},a}. \end{aligned} \tag{4}$$

Here, $S_{\text{homeCharging},a}$, $S_{\text{rangeAnxiety},a}$, $S_{\text{emptyBattery},a}$ and $S_{\text{walking},a}$ correspond to the behavioral terms introduced in UrbanEV, while $S_{\text{SoCdiff},a}$ is an end-of-horizon SoC shortfall term available in the EV Contrib or UrbanEV implementation. In our implementation, these EV specific terms are computed exactly as in the original UrbanEV framework and are left unchanged. The cost term $C_{\text{ch},a}$ is a new aggregate monetary component introduced in this study and is elaborated in Section 3.4. The inherited penalty, disutility, and reward components are instantiated as follows.

- *Home-charging reward:*

$$S_{\text{homeCharging},a} = \sum_{\mathcal{A}_a} \mathbb{I}\{\text{charging at a private home charger}\}, \tag{5}$$

  where $\mathcal{A}_a$ denotes the set of activities on agent a's daily plan and the indicator takes the value 1 if a private home charger is used and 0 otherwise. UrbanEV includes an optional home-charging indicator $S_{\text{homeCharging},a}$ (Eq. (5)). In the Gothenburg runs, we set $\beta_{\text{homeCharging}} = 0$ to avoid introducing a fixed home preference on top of explicit charger type tariffs.
- *Range anxiety penalty:*

$$S_{\text{rangeAnxiety},a}(t) = \max\left(0,\ \frac{\text{thres}_{\text{SoC},a} - \text{SoC}_a(t)}{\text{thres}_{\text{SoC},a}}\right), \tag{6}$$

  where $\text{SoC}_a(t)$ is the state of charge of EV agent a at time t and $\text{thres}_{\text{SoC},a}$ denotes the agent-specific range-anxiety threshold. In UrbanEV, this threshold ($\text{thres}_{\text{SoC},a}$) is read from a person attribute `rangeAnxietyThreshold` when present. If the attribute is absent in the population file, a global default value ($\text{thres}^{\text{def}}_{\text{SoC}}$) from the configuration is used as a fallback. During scoring, the instantaneous SoC trajectory is compared only to this agent-level threshold. This specification follows the UrbanEV formulation and approximates drivers' risk aversion against running close to their individual critical SoC level by assigning increasing disutility as $\text{SoC}_a(t)$ approaches $\text{thres}_{\text{SoC},a}$. The instantaneous, dimensionless indicator $S_{\text{rangeAnxiety},a}(t) \in [0,1]$ is evaluated whenever SoC changes and accumulated along the realised trajectory to form the aggregate term $S_{\text{rangeAnxiety},a}$ entering the scoring in Eq. (4).
- *Battery depletion penalty:*

$$S_{\text{emptyBattery},a}(t) = \mathbb{I}\{\text{SoC}_a(t) = 0\} \in \{0,1\}, \tag{7}$$

  which is multiplied by $\beta_{\text{emptyBattery}}$ in the scoring function and is only active when an agent fully depletes the battery. As in UrbanEV, this binary indicator acts as a strong deterrent against infeasible or highly undesirable plans that would leave the battery empty at any point along the day. We deliberately retain this large negative *soft* penalty, rather than enforcing a hard SoC constraint, to keep the co-evolutionary day-to-day search numerically robust while still making such plans effectively unacceptable in equilibrium.
- *Walking disutility:*

$$S_{\text{walking},a}(t) = 1 - \exp\left(-\lambda_{\text{walk}}\, d_{\text{walk},a}(t)\right), \qquad \lambda_{\text{walk}} > 0, \tag{8}$$

  where $d_{\text{walk},a}(t)$ is the straight-line walking distance between the charger and the activity location. In the implementation, we set $\lambda_{\text{walk}} \approx 0.005\ \text{m}^{-1}$ so that the penalty saturates for walking distances on the order of a few hundred meters (comparable to the maximum acceptable walking radius of $d_{\text{walk,max}} = 500\,\text{m}$). This term is multiplied by β_{walk} in the plan score. Here, λ_{walk} controls the saturation rate of the distance penalty with increasing $d_{\text{walk},a}(t)$, while β_{walk} scales the overall magnitude of walking-related disutility in the plan score. This functional form is consistent with the UrbanEV specification and captures the diminishing marginal disutility of walking as distance increases toward the maximum tolerated access radius.

- *End-of-horizon SoC shortfall penalty:*

$$S_{\text{SoCdiff},a} = \max\left(0,\ \text{SoC}_{\text{start},a} - \text{SoC}_{\text{end},a}(T)\right), \tag{9}$$

where $\text{SoC}_{\text{start},a}$ is the initial state of charge of vehicle a at the beginning of the simulation horizon and $\text{SoC}_{\text{end},a}(T)$ is its state of charge at the final simulation time T. This utility term is applied once per agent and penalizes only those agents whose terminal SoC falls below their initial SoC, via the coefficient β_{SoCdiff} in Eq. (4). In the EV Contrib/UrbanEV implementation, this SoC difference component is available as an optional multi-day behaviour term. We use it here as a simple proxy for forward-looking behaviour over the multi-day horizon, discouraging systematic end-of-horizon battery depletion without enforcing a hard SoC constraint or dominating the range anxiety and empty-battery penalties.

The EV specific utilities introduced here are retained from the UrbanEV behavioral backbone and remain unchanged in functional form. The following subsections focus on the methodological contributions of this research, which is the integration with charger-type-specific monetary costs and ToU aware intra-activity start-time rescheduling within MATSim's replanning loop.

Algorithm 1 EV charging cost helper used by Algorithms 2 and 3.

Require: Per-kWh prices $c^{\text{home}}, c^{\text{work}}, c^{\text{public}}$
Require: ToU multiplier $M_{\text{ToU}}(t)$ (applied to home charging. For flat tariffs or non-home chargers, $M_{\text{ToU}}(t) = 1$)

```
function ChargingCost(E_ch, type, t)                    ▷ E_ch in kWh, type ∈ {home, work, public}
    if type = home then
        c ← c^home
    else if type = work then
        c ← c^work
    else if type = public then
        c ← c^public
    else
        c ← 0                                           ▷ no monetary effect if type is unknown
    end if
    if type = home then
        m̃ ← M_ToU(t)
    else
        m̃ ← 1                                           ▷ currently no ToU variation for work / public
    end if
    C_ch ← E_ch × c × m̃                                 ▷ monetary charging cost
    return C_ch
end function
```

3.4. Cost aware charging behavior

Building on the EV augmented scoring formulation in Eq. (4), this work adds an explicit monetary charging-cost term that varies by charger type and by ToU profile. This extension allows agents to perceive heterogeneous charging prices at home, work, and public locations and to adapt their charging decisions accordingly. The monetary contribution enters the EV plan score as $\alpha_{\text{scaleCost}}\beta_{\text{money}}C_{\text{ch},a}$, where $C_{\text{ch},a}$ denotes the realised total monetary charging expenditure of agent a over the simulation horizon. Operationally, this total is accumulated session-wise during scoring: each realised charging session contributes a monetary increment $\Delta C_{\text{ch},a}(t)$ at its effective start time t, which is immediately converted into a score increment and added via MATSim's additive scoring interface. In conceptual terms, β_{money} is calibrated relative to the marginal disutility of travel time in the underlying MATSim configuration, so that charging costs are behaviorally relevant but remain comparable in magnitude to time and SoC related utilities, while $\alpha_{\text{scaleCost}}$ provides a calibrative scaler to adjust overall cost sensitivity without modifying the core setup.

For each completed charging session, the energy actually charged $E_{\text{ch},a}(t)$ [kWh], the charger type, and the effective charging start time t are recorded. Each sessions charging cost is defined as follows.

$$\Delta C_{\text{ch},a}(t) = E_{\text{ch},a}(t) \times c^{\kappa} \times M^{\kappa}_{\text{ToU}}(t), \tag{10}$$

where $\Delta C_{\text{ch},a}(t)$ denotes the session level monetary cost increment at effective charging start time t, $\kappa \in \{\text{home, work, public}\}$ denotes the charging access class, c^{κ} is the corresponding base tariff [currency/kWh], and $M^{\kappa}_{\text{ToU}}(t)$ is an access-class-specific, dimensionless time multiplier evaluated at t. In the present scenarios, time variation is applied only to home charging, such that $M^{\text{home}}_{\text{ToU}}(t) = M_{\text{ToU}}(t)$ and $M^{\text{work}}_{\text{ToU}}(t) = M^{\text{public}}_{\text{ToU}}(t) = 1$. Accordingly, $\Delta C_{\text{ch},a}(t) = E_{\text{ch},a}(t)\, c^{\kappa}$ for work and public sessions, and $\Delta C_{\text{ch},a}(t) = E_{\text{ch},a}(t)\, c^{\text{home}}\, M_{\text{ToU}}(t)$ for home sessions.

The total realized charging expenditure $C_{\text{ch},a}$ in Eq. (4) is obtained by accumulating $\Delta C_{\text{ch},a}(t)$ over all charging sessions of agent a across the simulation horizon. The residential multiplier $M_{\text{ToU}}(t)$ is constructed from an externally observed day-ahead price series. The data source and the derived hourly profile are described in Section 4.4.

Algorithm 2 Cost aware EV charging utility update (per charging session).

Require: Money-to-utility factor $\beta_{\text{money}} < 0$, scaling factor $\alpha_{\text{scaleCost}}$
Require: Stream of `ChargingBehaviourScoringEvent` instances emitted by handler

for all events e of type `ChargingBehaviourScoringEvent` **do**
  $(p, \text{type}, E_{\text{ch}}, t_{\text{price}}, \text{costOnly}) \leftarrow$ extract from e ▷ p = person; type ∈ {home, work, public}
  $U_\Delta \leftarrow 0$
  if $E_{\text{ch}} > 0$ **and** type ≠ `null` **then**
    if t_{price} is defined **then**
      $t \leftarrow t_{\text{price}}$ ▷ start time of actual charging (immediate or deferred)
    else
      $t \leftarrow e.\text{time}$ ▷ fallback: activity end time
    end if
    $\Delta C_{\text{ch}} \leftarrow \textsc{ChargingCost}(E_{\text{ch}}, \text{type}, t)$ ▷ Algorithm 1; returns session cost increment
    $U_\Delta \leftarrow \alpha_{\text{scaleCost}} \times \beta_{\text{money}} \times \Delta C_{\text{ch}}$
  end if
  if $U_\Delta \neq 0$ **then**
    add U_Δ to agent p's total plan score
    optionally log $(p, \text{type}, E_{\text{ch}}, t, \Delta C_{\text{ch}}, U_\Delta)$
  end if
  if not e.costOnly **then**
    apply remaining UrbanEV utilities
    (range anxiety, empty battery penalty, walking disutility, SoC difference penalty)
  end if
end for

In the implementation, the session level energy $E_{\text{ch},a}(t)$ is obtained from the realized SoC change over the charging activity and the vehicle's usable battery capacity as simulated by EV Contrib, so that the monetary cost reflects the actual energy taken on during that stop and thus depends on the agent's prior trip sequence and SoC trajectory. The framework does not introduce a separate, explicit disutility for splitting charging into multiple sessions. Instead, fragmented charging is implicitly penalized through repeated access and walking disutility, any additional in-vehicle travel time associated with reaching chargers, the accumulation of monetary expenditure across all sessions, and the range anxiety and SoC differential penalties if repeated small top-ups leave the vehicle frequently close to the anxiety threshold or systematically depleted at the end of the horizon. As the cost scoring and ToU rescheduling procedures constitute the primary methodological contribution, their pseudocode is provided here.

Introducing an additional generic per session penalty would require dedicated behavioral data for identification and is therefore not pursued here. Each realized charging session's monetary increment $\Delta C_{\text{ch},a}(t)$ is converted into an incremental utility contribution that is applied at scoring time.

$$\Delta U_{\text{cost},a}(t) = \alpha_{\text{scaleCost}} \times \beta_{\text{money}} \times \Delta C_{\text{ch},a}(t), \tag{11}$$

and these increments are accumulated over the horizon to yield the compact cost term $\alpha_{\text{scaleCost}}\beta_{\text{money}}C_{\text{ch},a}$ appearing in Eq. (4). Accordingly, Eq. (11) specifies the per session scoring update used to construct $C_{\text{ch},a}$, rather than an additional monetary term applied on top of Eq. (4). In the implementation, a charging behaviour scoring component listens to scoring event instances and applies $\Delta U_{\text{cost},a}(t)$ using the effective charging start time t (immediate or deferred) carried by the handler.

3.5. Adaptive smart charging logic and rescheduling mechanism

The adaptive smart charging logic embedded within the EV agent decision process, integrating spatial charger availability, SoC thresholds, and cost minimization, is elaborated here. This extension decouples plug-in time from charging start time for a subset of agents and activities, enabling probabilistic smart-charging behaviour that responds to time-of-use (ToU) tariffs while remaining constrained by range anxiety and charger availability. Fig. 2 summarizes the resulting decision flow. During the *mobsim* routine, each EV agent's SoC is updated event by event. When an agent reaches a potential charging opportunity, the framework evaluates SoC, the remaining trip chain, and local charger availability within the same utility based scoring environment used for UrbanEV's original charging logic.

In range-critical situations, where current SoC falls below the individual range anxiety threshold or is insufficient for the next planned trip, the low-SoC and empty-battery penalties dominate the plan score. The flow therefore collapses to immediate charging at the nearest feasible charger, typically a public or workplace facility, regardless of price. Deferred, cost-minimizing home charging is only considered when the agent is parked at home, the current SoC is safely above the range anxiety threshold, and the planned dwell time exceeds the required charging duration. In these cases, the home-charging handler computes the plug-in window from activity start and end times, evaluates the ToU multipliers over this window, and selects a cost-minimizing charging start time subject to these constraints.

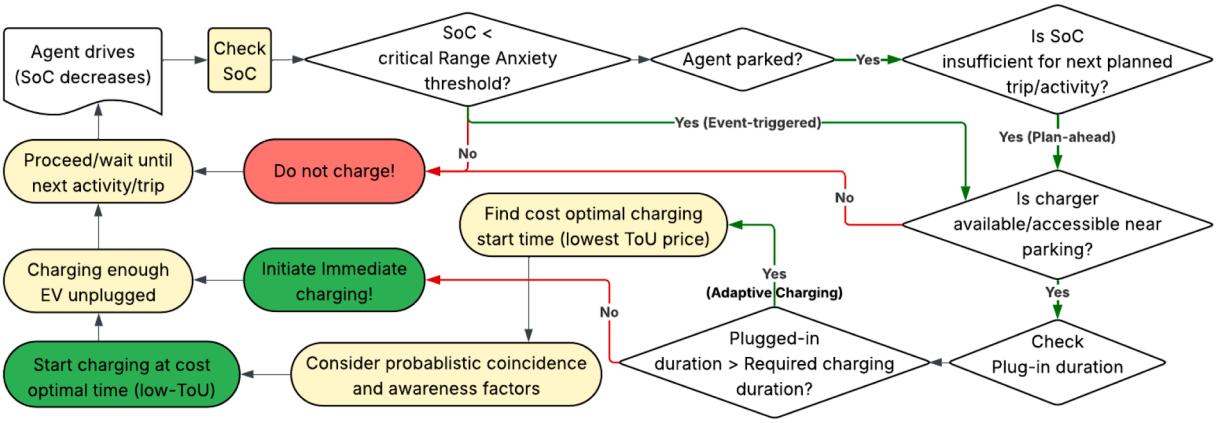

Fig. 2. Decision flow for EV charging within the extended UrbanEV framework.

Compliance with smart charging is heterogeneous and implemented through a two-stage mechanism. First, only a ToU-aware subpopulation is eligible for deferral: at initialisation, agents are assigned the binary attribute `smartChargingAware` with probability f_{aware}, and only these agents evaluate ToU information when parked at home with a feasible plug-in window. Second, even when deferral is feasible, imperfect compliance is introduced via the coincidence factor f_{coinc}, which probabilistically overrides the optimiser and reverts the session to immediate charging at arrival. Operationally, for eligible home stops the handler searches over the feasible start-time set $\mathcal{T}$ (Eq. (12)) and selects $t^{\star}_{\text{start}}$ by minimizing the proxy objective $J(t)$ (Eq. (13)); the mechanics are given in Algorithm 3. This design yields a mix of delayed and immediate starts without hard coding deterministic synchronization at ToU minima.
For agents marked as ToU aware at eligible home activities, the handler estimates the energy required to approximately fill the battery during the current stop, E_{req}, and approximates the corresponding charging duration T_{ch} using the configured home-charger power. If the available plug-in window satisfies $t_{\text{dep}} - t_{\text{arr}} > T_{\text{ch}}$, deferred charging is considered feasible. Otherwise, the vehicle is plugged in immediately upon arrival. For feasible cases, a helper routine performs a grid search over candidate start times.

$$t \in \mathcal{T} = \{t_{\text{arr}},\ t_{\text{arr}} + \Delta t,\ \ldots,\ t_{\text{dep}} - T_{\text{ch}}\}, \tag{12}$$

with step size Δt (15 minutes). For each candidate $t \in \mathcal{T}$, it evaluates a proxy objective $J(t)$ proportional to the effective home-charging price. Since E_{req} and c^{home} are constant across candidates within the same plug-in window, minimizing $J(t)$ is equivalent to minimizing the monetary session cost. The cost minimizing start time is then selected.

$$t^{\star}_{\text{start}} = \arg\min_{t \in \mathcal{T}} \{J(t)\}, \tag{13}$$

In Algorithm 3, $J(t)$ is implemented as the ToU multiplier $M_{\text{ToU}}(t)$, with optional temporal scaling $M_{\text{ToU}}(t)^{\alpha_{\text{scaleTemporal}}}$ applied in the evening window. The scaling mechanism ($\alpha_{\text{scaleTemporal}}$) increases the likelihood that cost minimizing start times fall into low-tariff night hours, while leaving the empirical $M_{\text{ToU}}(t)$ profile intact. If $|t^{\star}_{\text{start}} - t_{\text{arr}}| \leq 60$ s, the optimum is treated as equivalent to immediate charging and the EV is plugged in at t_{arr}. Otherwise, imperfect compliance is applied. With probability f_{coinc} the cost minimising deferral is ignored and charging starts immediately at arrival, and with probability $1 - f_{\text{coinc}}$ the vehicle's plug-in is deferred to the cost minimizing start time $t^{\star}_{\text{start}}$. The coincidence factor is the probability of overriding the optimizer (immediate charging), and it reduces excessive synchronization of charging starts at ToU minima. In all cases, the handler records the SoC trajectory and the effective charging start time for use by the cost scoring module. The cost aware and smart-charging extensions are embedded within the existing UrbanEV architecture. The framework manages charger selection, physical plug-in and unplugging, and, where applicable, the smart scheduling of deferred home charging. A smart charging scheduler enforces the deferred plug-in times $t^{\star}_{\text{start}}$ and ensures that the realised power profiles follow the configured charging curves once charging begins. At the end of each charging activity, the handler computes the realised energy intake and emits a *Scoring* event containing the energy, charger type, and effective charging start time. During scoring, charging behaviour scoring module evaluates the monetary cost term alongside the inherited EV specific utilities, and the resulting $S_{\text{EV,plan},a}$ feeds into MATSim's standard replanning loop. In the present implementation, activity locations are taken as fixed by the input plans, while route choice (and limited departure-time adjustment, where enabled) is handled through MATSim's iterative scoring and replanning. In the Gothenburg configuration used here, the smart charging extension operates strictly at the intra-activity level. It selects a home charging start time within a fixed home activity parked window and does not directly alter activity end times or first morning departure times. Any feedback from deferral into departure time or route patterns can therefore only arise indirectly through MATSim's standard co-evolutionary replanning responding to changed EV plan scores. In this sense, deferral affects travel behavior only through the induced SoC trajectory and the resulting range anxiety, empty battery, and SoC difference penalties, rather than through explicit schedule control. For the present scenarios, a discernible systematic shift in the aggregate distribution of first morning car departure times between cost aware immediate charging and adaptive smart charging are not observed. The dominant effect is the temporal reshaping of home charging within the plug-in window.

Algorithm 3 Smart ToU aware home charging with temporal scaling.

Require: UrbanEV config cfg with:
enableSmartCharging, $f_{\text{coinc}} \in [0, 1]$, $\alpha_{\text{scaleTemporal}} \geq 1$, home-charger power P_{home}
Require: person flag `smartChargingAware` $\in$ {true,false}

procedure HANDLEHOMECHARGINGSTART($p, ev, a, t_{\text{arr}}, cfg$)
  if a.type $\neq$ "home charging" **then**
    plug in immediately at t_{arr}; store start SoC/time; **return**
  end if
  $charger \leftarrow$ closest feasible charger for ev at location(a)
  if $charger = \emptyset$ **then**
    mark a as "failed charging"; **return**
  end if
  $t_{\text{dep}} \leftarrow$ planned end time of a (if missing: t_{arr})
  if $t_{\text{dep}} \leq t_{\text{arr}}$ **then**
    plug in immediately; store start SoC/time; **return**
  end if
  aware $\leftarrow$ (p.smartChargingAware = `true`)
  if not cfg.enableSmartCharging **or not** aware **then**
    plug in immediately; store start SoC/time; **return**
  end if
  $E_{\text{req}} \leftarrow$ energy missing to (approx.) charge battery during this stop
  $T_{\text{ch}} \leftarrow E_{\text{req}} / P_{\text{home}} \times 3600$ ▷ duration [s]
  if $T_{\text{ch}} \leq 0$ **or** $t_{\text{dep}} - t_{\text{arr}} \leq T_{\text{ch}}$ **then**
    plug in immediately; store start SoC/time; **return**
  end if
  $t_{\text{max}} \leftarrow t_{\text{dep}} - T_{\text{ch}}$, $\Delta t \leftarrow 900$ s
  $t^{\star} \leftarrow t_{\text{arr}}$, $J^{\star} \leftarrow +\infty$
  for $t = t_{\text{arr}}$ **to** t_{max} **step** Δt **do**
    $\tau \leftarrow (t \bmod 86400)/3600$; $m \leftarrow M_{\text{ToU}}(t)$
    if $17 \leq \tau < 22$ **then**
      $m \leftarrow m^{\alpha_{\text{scaleTemporal}}}$ ▷ temporal scaling in search
    end if
    if $m < J^{\star}$ **then**
      $J^{\star} \leftarrow m$, $t^{\star} \leftarrow t$
    end if
  end for
  draw $r \sim U(0, 1)$
  if $r < f_{\text{coinc}}$ **then**
    $t^{\star} \leftarrow t_{\text{arr}}$ ▷ override optimizer: immediate charging
  end if
  if $|t^{\star} - t_{\text{arr}}| \leq 60$ s **then**
    plug in immediately; store start SoC/time
  else
    schedule deferred plug-in of ev at $charger$ for $t^{\star}$
  end if
end procedure

The smart charging module operates at the intra-activity level by shifting home charging start times within the existing dwell window, without directly modifying activity schedules. The feedback arises indirectly through the resulting SoC trajectory and associated EV specific utilities. Plans that defer excessively and therefore arrive at morning commutes with low SoC, require additional emergency charging, or end the horizon with systematically depleted batteries receive lower EV plan scores and are selected less frequently in the co-evolutionary loop. But by combining UrbanEV's multi-criteria charging behavior with the cost aware and ToU aware extensions described above, the model generates emergent, heterogeneous patterns of charging deferral and peak shifting without prescribing ex-ante charging schedules. This explicit linkage between dynamic tariffs, the awareness and coincidence factors, and plan based charging decisions is central to the peak-demand and infrastructure implications analyzed in the subsequent sections. In combination with the weekly simulation horizon, this iterative replanning loop therefore represents forward-looking behavior in a bounded rational form, without requiring explicit multi-day dynamic programming of SoC trajectories. The numerical values of

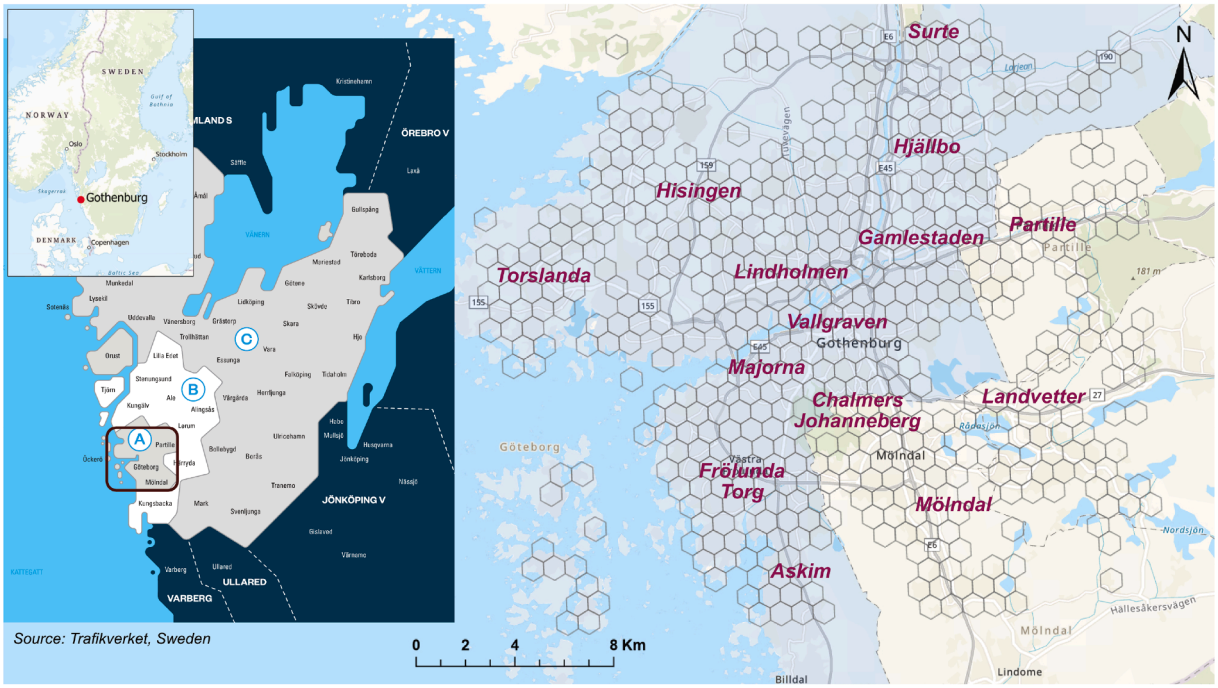

Fig. 3. Study area (Region A, Trafikverket) within Greater Gothenburg, Sweden, with key zones.

behavioral, infrastructure, and tariff parameters are scenario-specific. The Gothenburg region instantiation and calibration used in this study are reported with specific case relevant inputs in Section 4, with a detailed discussion in Section 4.6 (Table 4).

4. Data and study area: gothenburg region, sweden

The simulated spatiotemporal charging demand and travel behavior in MATSim require integrating synthetic activity travel demand, a multimodal transport network, EV specifications, charging infrastructure, and dynamic electricity pricing. The study focuses on Trafikverket's demarcated Region A in the Gothenburg metropolitan area, comprising Gothenburg and the adjacent municipalities of Partille and Mölndal. This region defines the spatial boundary for the synthetic population, transport network, and charger datasets used in the simulation. The urban core of Gothenburg is characterized by dense development and extensive public transit networks, while suburban areas exhibit higher reliance on private vehicles. The distribution of charging infrastructure is strategically aligned with population density, employment centers, and traffic flows, ensuring comprehensive coverage across residential, commercial, and transit hubs.

4.1. Synthetic population and trip activity patterns

To model near-future scenarios, we assume a 50 % EV adoption rate within the region. The synthetic population data is sourced from the Synthetic Sweden Mobility (SySMo) model (Tozluoglu et al., 2023), which synthesizes socio-demographic information from Statistics Sweden, the national travel survey, and origin-destination matrices from the Sampers model (Parishwad and Jia, 2023). This dataset comprises 557,220 individuals, each with detailed demographic attributes, including age, gender, employment status, income levels, and residential locations. Daily activity chains are assigned to each agent, detailing sequences of activities (such as home, work, and shopping) with specified start and end times, durations, and travel modes. For this study, 211,880 individuals are designated as car users, with 105,940 randomly assigned as EV users, reflecting a projected 50 % penetration rate. All population and fleet counts reported in this section, including the EV counts in Table 1, are stated for the full population with 50 % EV adoption scenario. For computational tractability, the MATSim runs are executed on a 10 % sample, and reported charging demands and the derived totals are scaled by the inverse sampling factor to represent the entire population.

4.2. Electric vehicle specifications

The labels reported in Table 1 are used as archetype identifiers in the simulation inputs and are retained for readability. They should not be interpreted as exact manufacturer trim specifications. Energy consumption, usable battery capacity, and maximum C-rate are therefore selected to cover a representative range of EV performance under European driving conditions rather than to

Table 1
Simulated vehicle types and charging-relevant parameters.

Archetype Model	Energy [kWh/100 km]	Battery [kWh]	C-rate Max[C]	Max DC [kW]	Max AC power H/W/P [kW]	Count
BMW i3	21.0	42	2.0	84	7 / 11 / 22	22 050
Renault ZOE	17.2	52	1.5	78	7 / 11 / 22	21 260
Tesla Model Y	18.3	75	2.0	150	7 / 11 / 22	20 640
Volvo	15.6	60	1.5	90	7 / 11 / 22	21 070
VW ID.4†	16.3	34	2.0	68	7 / 11 / 22	20 920

Table 2
Simulated charger infrastructure.

Type	Nominal power	Plugs per station	Stations	Utilised stations
Home	7 kW	1	8475	7737
Work	11 kW	1	8475	3204
Public	22 kW	10	796	662

Table 3
Aggregate ToU multipliers.

Time window	Multiplier	Charging cost
00:00-06:00	0.70	Low
06:00-08:00	1.60	High
08:00-10:00	1.47	High
10:00-17:00	0.92	Medium
17:00-20:00	1.14	High
20:00-22:00	1.00	Medium
22:00-24:00	0.70	Low

reproduce any single commercial configuration. The dagger (†) marks an intentionally stylized label, included to represent a smaller archetype. The ID.4 variants are typically offered in substantially larger battery capacity than the 34 kWh value used here.

The initial SoC for EVs is randomly set between 60 % and 80 %, reflecting typical user behavior and ensuring variability in charging needs. Agents are also assigned attributes influencing charging decisions, including range anxiety thresholds and charger-accessibility indicators, which govern when and where charging is selected under the co-evolutionary scoring and replanning loop.

4.3. Charging infrastructure and accessibility

Charging infrastructure is categorized into home, workplace, and public chargers, each with distinct power outputs: 7 kW for home chargers, 11 kW for workplace chargers, and 22 kW for public chargers. In this near-future scenario, we assume an 80 % availability of home and workplace chargers, randomly assigned to agents based on their residential and employment locations. The spatial distribution of public chargers is optimized to align with residential density, employment hubs, and prevalent travel patterns, ensuring accessibility and convenience for EV users.

Public charging is represented at the access charger and AC power levels using a single tariff per charger, for the study's abundant capacity assumption, as discussed in Section 3. Queuing and station specific price heterogeneity are not modeled, as the focus is unconstrained, behaviorally consistent demand surfaces rather than station level operations (Section 6).

4.4. Dynamic electricity pricing

Electricity pricing data is integrated to reflect real-world cost variations and influence charging decisions. Hourly day-ahead area prices for the SE3 bidding zone are obtained from Nord Pool's market data portal (Nord Pool, 2024) and converted to SEK/kWh. The ToU signal is implemented as a dimensionless multiplier $M_{\mathrm{ToU}}(t)$ by constructing a representative hourly profile and normalizing it to unit mean. Specifically, day-ahead area prices for SE3 are aggregated to an hourly series, and then averaged across the analysis year to obtain a representative 24-hour profile. The resulting vector is normalized to define $M_{\mathrm{ToU}}(t)$. This multiplier is applied to the base home charging tariff in the charging cost term (Section 3.4), while work and public tariffs are treated as flat in time in the present scenarios (equivalently, $M_{\mathrm{ToU}}(t) \equiv 1$ for those work and public classes).

Any such non-energy components in real-world tariffs would need to be folded into an effective SEK/kWh rate in future extensions. Incorporating dynamic pricing via $M_{\mathrm{ToU}}(t)$ enables the simulation to capture EV users' economic considerations, as they may adjust their charging behavior to take advantage of lower-cost periods, thereby influencing overall charging demand patterns Table 2.

Table 4
UrbanEV simulation and configured parameters (Gothenburg case study).

Parameter	Value	Parameter	Value	Parameter	Value
T_{sim}	168 h	$N_{\text{maxChanges}}$	2	$p_{\text{replan,nonCrit}}$	0.3
p_{timeAdj}	0.1 [10 %]	$\text{thres}_{\text{SoC}}^{\text{def}}$	0.2 [20 %]	t_{flex}	600 [s]
λ_{walk}	0.005 [m^{-1}]	β_{walk}	–1.0 [utils]	β_{SoCdiff}	–4.0 [utils]
$\beta_{\text{rangeAnxiety}}$	–6.0 [utils]	$\beta_{\text{emptyBattery}}$	–15.0 [utils]	$\beta_{\text{homeCharging}}$	0 [utils]
c^{home}	2.5 [kr/kWh]	c^{work}	4.0 [kr/kWh]	c^{public}	5.5 [kr/kWh]
β_{money}	–0.05 [util/kr]	$\alpha_{\text{scaleTemporal}}$	0.5	$\alpha_{\text{scaleCost}}$	1.0
$s_{\text{smartCharging}}$	true	f_{aware}	0.3 [30 %]	f_{coinc}	0.7 [70 %]

4.5. Transport network integration

The simulation environment incorporates a detailed transport network, including road infrastructure and public transit schedules. Road attributes such as free-flow speeds, capacities, and allowed modes are derived from OpenStreetMap and supplemented with additional data to enhance accuracy (Moeckel et al., 2020). Consistency for the coordinate system (EPSG:3006) was maintained across spatial datasets. Public transport schedules for buses, trams, ferries, and rail services are integrated to enable the modeling of multimodal travel behaviors. This comprehensive network representation is essential for accurately simulating route choices, travel times, and interactions between different transport modes (Zhuge et al., 2021).

4.6. Behavioral utility parameters

Several utility and configuration parameters in Table 4 are not directly observable, yet they govern how agents trade off charging cost, accessibility, and battery-related risk within the deployed co-evolutionary replanning loop. Their magnitudes were anchored in the published UrbanEV configuration and then adjusted only insofar as required to obtain behaviorally plausible charging initiation SoC levels and a realistic (non-universal) response to time-varying residential electricity prices. The resulting parameterization is treated as a consistent scenario configuration for Gothenburg rather than a unique, statistically identified estimate, and the same calibration logic can be transferred to other regions given local value-of-time evidence, electricity price profiles, and observed charging traces. The multi-day simulation horizon is set to $T_{\text{sim}} = 168$ h to cover a continuous week. This horizon length allows weekly charging routines to emerge and enables the end-of-horizon SoC shortfall term to regularize inter-day SoC trajectories. Co-evolutionary learning intensity is controlled via the maximum number of daily plan changes and the replanning probability for non-critical agents, while schedule realism is maintained through bounded activity-time flexibility (t_{flex} and p_{timeAdj}). Spatial feasibility and access frictions are controlled through the charger search radius d_{search} and the associated walking disutility, which together regulate the willingness to use off-route chargers around an activity location.

Battery-related preferences follow the agent-specific UrbanEV formulation. Each EV agent carries a `rangeAnxietyThreshold` attribute, interpreted as the SoC level below which disutility rises sharply and charging becomes increasingly preferred. In the Gothenburg population, this attribute is instantiated for all EV users by sampling thresholds in the range 0.15 to 0.30 of usable battery capacity, capturing heterogeneity in risk tolerance. The configuration value $\text{thres}_{\text{SoC}}^{\text{def}}$ reported in Table 4 acts only as a fallback if the person attribute is absent and is not used when `rangeAnxietyThreshold` is specified. With this setup, the scoring compares each vehicle's instantaneous SoC only to its own threshold, and the simulated SoC at charging initiation is concentrated around this band with only a small tail of very low-SoC events, consistent with empirical evidence that most users initiate charging well before complete depletion (Sun et al., 2015; Ge and MacKenzie, 2022). The inherited empty-battery penalty is retained as a strong deterrent against infeasible plans, while the home-charging reward coefficient is set to $\beta_{\text{homeCharging}} = 0$ so that any preference for home charging arises endogenously from tariffs and ToU structure rather than from an additional fixed bonus. Monetary sensitivity is specified through the marginal utility of money and the charger-type tariffs. Distinct base prices $c^{\text{home}}, c^{\text{work}}, c^{\text{public}}$ encode a cost hierarchy across access contexts, while the residential time-of-use signal is implemented through a normalized multiplier $M_{\text{ToU}}(t)$ derived from externally observed day-ahead prices for the relevant bidding zone (Nord Pool, 2024). The monetary term introduced in this work converts realised charging expenditures into utility via $\alpha_{\text{scaleCost}}\beta_{\text{money}}$ (Methods, Eq. (4)). To keep monetary incentives commensurate with MATSim's behavioural time scale, β_{money} is anchored using a locally relevant value-of-travel-time savings. Swedish appraisal and congestion-pricing evidence suggests that car users' values of time are on the order of ~60–120 SEK/h for private travel (Börjesson and Eliasson, 2014). With a representative car travel-time marginal utility $\beta_{\text{trav,car}} = -6$ utils/h in the MATSim configuration, indifference between one additional hour of car travel and paying V SEK implies a feasibly adopted, imminent value of $\beta_{\text{money}} = -0.10$ utils/SEK so that typical intra-day price spreads (tens of SEK per session) remain behaviorally salient, yet do not dominate activity and travel utilities.

$$\left|\beta_{\text{money}}\right| \approx \frac{\left|\beta_{\text{trav,car}}\right|}{V} \in \left[\frac{6}{120}, \frac{6}{60}\right] = [0.05,\ 0.10]\ \text{utils/SEK}.$$

In this calibration, shifting a home charging session between low and high price hours produces utility changes comparable to a few minutes of car travel time. The purely technical scaling factor is kept at $\alpha_{\text{scaleCost}} = 1.0$, so that overall price responsiveness is governed primarily by β_{money} rather than by an additional multiplier.

Adaptive smart charging behavior is regulated by three behavioral controls that encode heterogeneous eligibility and imperfect compliance. First, the global smart-charging switch activates the ToU-aware rescheduling logic for home charging. Second, an aware-

ness factor f_{aware} determines the share of agents that evaluate $M_{\text{ToU}}(t)$ when selecting a start time within the home plug-in window. Third, a coincidence (override) factor f_{coinc} forces a subset of technically feasible deferred sessions to start immediately upon arrival, preventing unrealistic synchronization at tariff minima and representing persistent plug-in-immediately behavior observed in practice (Ensslen et al., 2018; Rostami et al., 2024). Finally, temporal salience is represented via $\alpha_{\text{scaleTemporal}} = 2.0$, applied only within the rescheduling search objective (evening hours) to accentuate high-price periods in the selection of candidate start times. This mechanism modifies the perceived penalty in the optimizer while leaving the empirical ToU multiplier itself unchanged in the monetary cost calculation. Together, the awareness, coincidence, and temporal-salience controls are tuned such that the simulated home-charging profile exhibits partial but not universal migration into low-tariff night hours, a reduced yet non-zero early-evening peak, and plausible heterogeneity across users, while total daily energy demand remains primarily governed by mobility energy requirements rather than by tariff artifacts.

Overall, the Gothenburg parameter set in Table 4 preserves the UrbanEV scaling between SoC-related penalties, accessibility frictions, and MATSim travel and activity utilities, and it adds a monetary term and a probabilistic ToU-aware rescheduling mechanism that are feasibly calibrated to be behaviorally relevant at the weekly horizon. Post hoc checks on SoC-at-plug-in distributions and on the resulting off-peak home-charging share are used as plausibility diagnostics rather than as formal validation, given the absence of individual-level charging survey data for the full synthetic population.

5. Results and analysis

This section presents the outputs of the integrated ABM framework implemented based on MATSim. The simulations converge at 60 optimization iterations, as utilities of all agents stabilize, ensuring transport equilibrium. We begin by assessing the direct output, which involves tracking or recording individual SoC dynamics at 15-minute intervals, capturing both discharge during trips and charging events of each EV.

5.1. Estimated SoC dynamics of EVs

The key output is the high-resolution charging events of all the simulated EVs, including their SoC dynamics over time with location information. Fig. 4 presents one week of SoC trajectories for five randomly sampled vehicles (5-minute resolution). The piecewise-linear ramps identify charger types via their slopes: the steepest segments correspond to public charging (22 kW), followed by workplace (11 kW), and then home charging (7 kW). Effective ramp rates are slightly lower than nameplate due to charger-vehicle efficiency and taper behaviour represented in the fleet module, so observed slopes cluster just below their nominal values. This is consistent with measured AC charging efficiencies reported in the literature (Sevdari et al., 2023).

Agents start the simulation with an initial SoC uniformly drawn between 60–80 %, and an empty-battery penalty prevents trajectories from approaching zero. A cost term discourages unnecessary charging to 100 % unless upcoming trips require the energy, while the SoC-difference utility regularizes multi-day SoC trajectories so that vehicles do not systematically end the simulated week far below their initial SoC (Section 3.3). Across the week, daily SoC declines of approximately 5–15 kWh align with the assumed consumption rates (15.6-21 kWh/100 km) embedded in the vehicle model. Blue bands mark off-peak ToU windows (22:00-06:00). The smart charging module enables price-responsive rescheduling: home sessions are deferred by roughly 4–5 h into low-tariff periods (dot-dash overlays), evident on Days 1-3 and Day 4 in the zoomed panel (Fig. 4(b)). This systematic shift to off-peak hours mirrors empirical findings on ToU responsiveness among EV users. The zoomed view also highlights heterogeneous charging strategies driven by access and preferences. Vehicle 9512556 performs a single overnight home session (gain $\approx$ 25 kWh over $\sim$6 h), whereas others fragment charging into shorter bursts around activities, reflecting trade-offs among energy cost, schedule disruption, and walking disutility to charger nodes (Section 3.3). Vehicles with constrained home access (ID 5563501) exhibit intermittent public sessions when SoC approaches a driver-specific range anxiety threshold. Agents with reliable home access top up more consistently overnight. Such home-public asymmetries and user-specific session structures are in line with large-scale empirical analyses of charging behaviour (Zhan et al., 2025; Lin et al., 2021).

5.2. Temporal charging demand scenarios

The individual SoC trajectories for all agents were aggregated to hourly charging loads under three scenario settings (Fig. 5). In the baseline **Scenario 1 (Non-cost aware immediate charging)**, assuming no monetary charging costs (as many studies do), agents charge where and when it is most convenient (Fig. 5(a)). Workplace charging dominates the morning peak (06:00–09:00), reaching 32,012 kW at 07:00 and totaling 275,320 kWh over the day, driven purely by arrival convenience at the workplace (Novosel et al., 2015). Home charging shows a diurnal shape with a minimum of 3,254 kW at 08:00 and a peak of 34,576 kW at 17:00, summing up to 397,074 kWh. Public charging is relatively uniform (total 304,938 kWh; peak 23,614 kW at 10:00). The absence of considering charging cost produces pronounced workplace-arrival peaks and modest overnight residential charging, consistent with convenience-driven behavior seen in prior ABM studies (Yi et al., 2023).

In **Scenario 2 (Charger-cost aware immediate charging)** represented by Fig. 5(b), fixed work and public tariffs of 4.0 and 5.5 SEK/kWh, respectively (Table 4), are combined with ToU pricing at home (Table 3), which shifts energy toward cheaper home charging (Fig. 5(b)). Workplace demand still exhibits a pronounced morning peak (37,624 kW at 08:00; daily 186,352 kWh), while home charging rises to 540,678 kWh, by +36.2 % compared to Scenario 1, with a higher evening maximum of 50,306 kW at 18:00

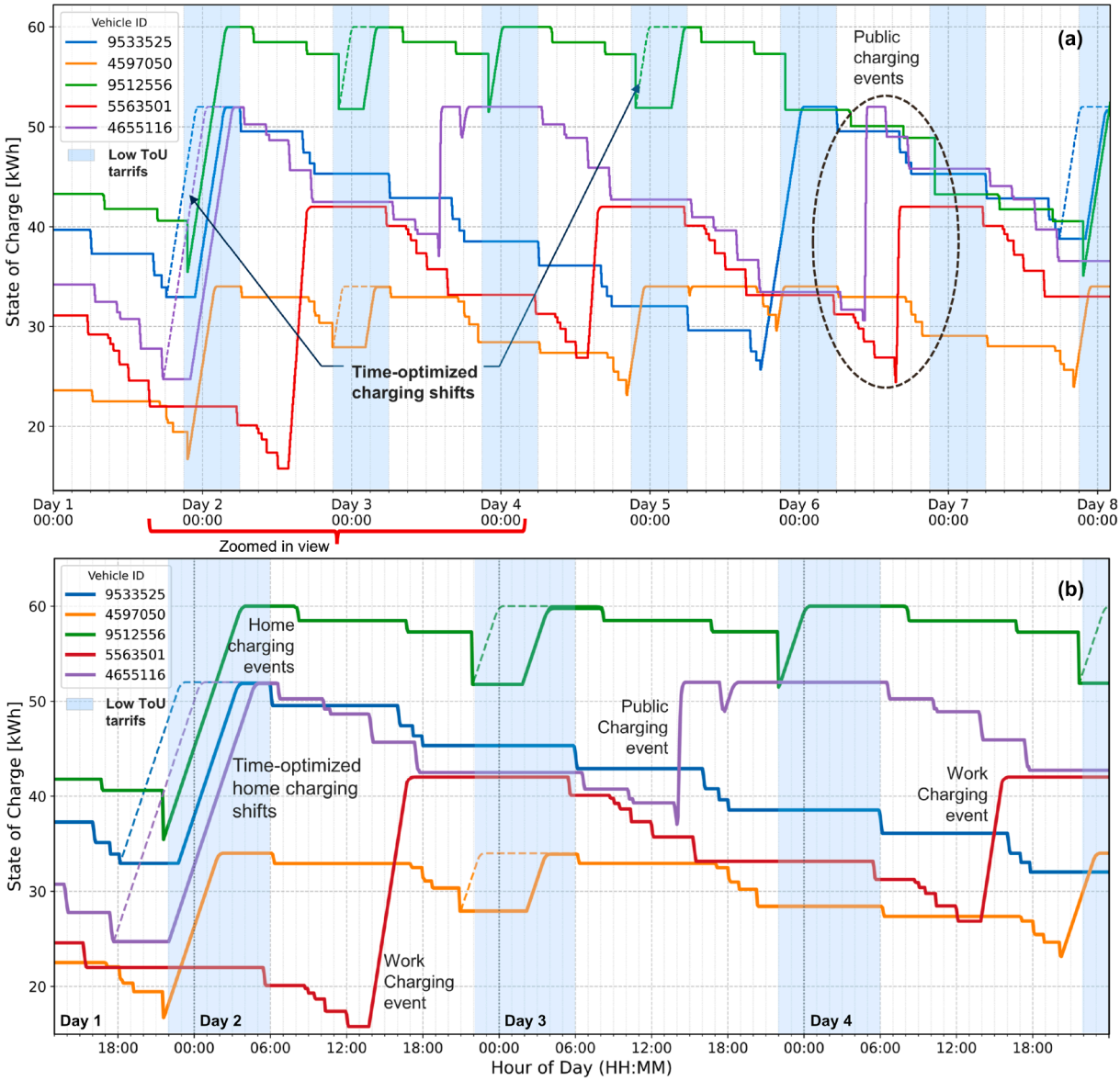

Fig. 4. (a) SoC trajectories for five EV agents over the simulated week (b) Zoomed view of SoC profiles.

(+45.5 % vs. Scenario 1). Public charging drops to 242,900 kWh (a reduction of 20.3 % compared to Scenario 1), indicating substitution away from costlier locations.

In **Scenario 3 (Adaptive cost aware smart charging)** represented by Fig. 5(c), allowing 70 % of agents to optimise start times within their plug-in windows (with a 30 % coincidence factor introducing stochastic lags) smooths the evening residential peak while preserving daytime accessibility (Fig. 5(c)). Daily workplace and public totals are 186,352 kWh and 242,900 kWh, being nearly unchanged relative to Scenario 2. Home charging increases slightly to 542,678 kWh (+0.37 % compared to Scenario 2). The residential peak attenuates from 50,306 kW in Scenario 2 (at 18:00) to 40,354 kW in Scenario 3 (at 16:00), corresponding to a reduction of about 19.8 % in the home peak relative to the cost aware immediate-charging baseline, while still remaining roughly 16.7 % above the convenience-driven peak in Scenario 1. Off-peak (22:00–06:00) home charging increases correspondingly, shifting additional demand into low-tariff hours. This behavior mirrors findings that randomized or probabilistic smart charging avoids rebound spikes at tariff boundaries and shifts load into low-price windows (Göberndorfer et al., 2024).

Fig. 5(d) summarizes daily energy: Scenario 1 totals 977,332 kWh (home 397,074 kWh; work 275,320 kWh; public 304,938 kWh), with roughly 40 % of the energy used at home and about 60 % at work and public chargers. Under charger-cost aware immediate charging (Scenario 2), the total is 969,930 kWh, with home charging increasing to 540,678 kWh (55.7 % of daily energy) and work and public use decreasing correspondingly. Adaptive smart charging (Scenario 3) yields 971,930 kWh total, keeping aggregate

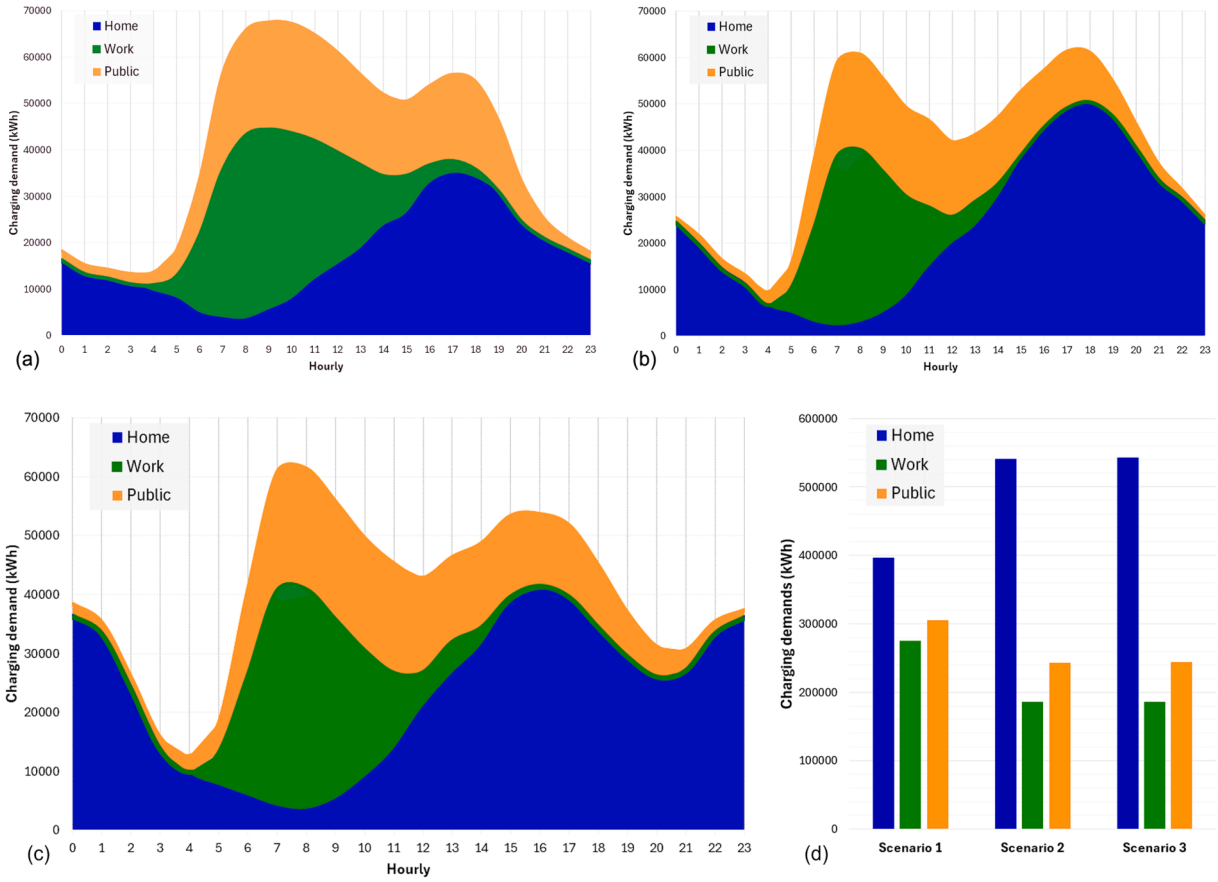

Fig. 5. Hourly aggregate charging demand by charger type (a) Scenario 1 (Non-cost aware immediate charging), (b) Scenario 2 (Charger cost aware immediate charging), (c) Scenario 3 (Adaptive cost aware smart charging), (d) Daily energy totals by scenario.

Table 5
Summary of hourly residential and system wide peak charging demands.

	Scenario 1 Non-cost aware immediate	Scenario 2 cost aware immediate	Scenario 3 Adaptive smart charging
Home peak [kW]	34 576	50 306	40 354
Home peak time [h]	17:00	18:00	16:00
System-wide peak [kW]	67 564	61 398	61 393
System-wide peak time [h]	09:00	17:00	08:00
Home peak shift vs. S1 [%]	0.0	+45.5	**+16.7**
Home peak shift vs. S2 [%]	–31.3	0.0	**–19.8**

consumption within about 1 % of Scenario 1 but materially altering the temporal allocation. Table 5 summarizes the resulting hourly home peaks and their relative changes across scenarios. For the Gothenburg case, introducing charger-cost awareness with ToU tariffs (Scenario 2) increases the residential peak from 34,576 kWh/h at 17:00 (Scenario 1) to 50,306 kWh/h at 18:00 (+45.5 %). Activating adaptive smart charging (Scenario 3) then reduces this peak to 40,354 kWh/h at 16:00 (about −19.8 % relative to Scenario 2 and +16.7 % relative to Scenario 1).

Together, these results demonstrate how utility based and price-responsive charging strategies within an ABM framework can alter aggregate demand profiles, shifting residential load into off-peak intervals while maintaining workplace and public charging patterns. The subsequent section spatially disaggregates these temporal outcomes to reveal geographic charging hotspots and infrastructure utilization across the Gothenburg region.

5.3. Spatial patterns of charging demand and utilization

Fig. 6 presents hexagonally aggregated daily charging metrics across Gothenburg Region A (see Fig. 3). The aggregation employs a regular hexagonal grid with an area of approximately 1 km^2 per cell, which provides neighbourhood-scale resolution while main-

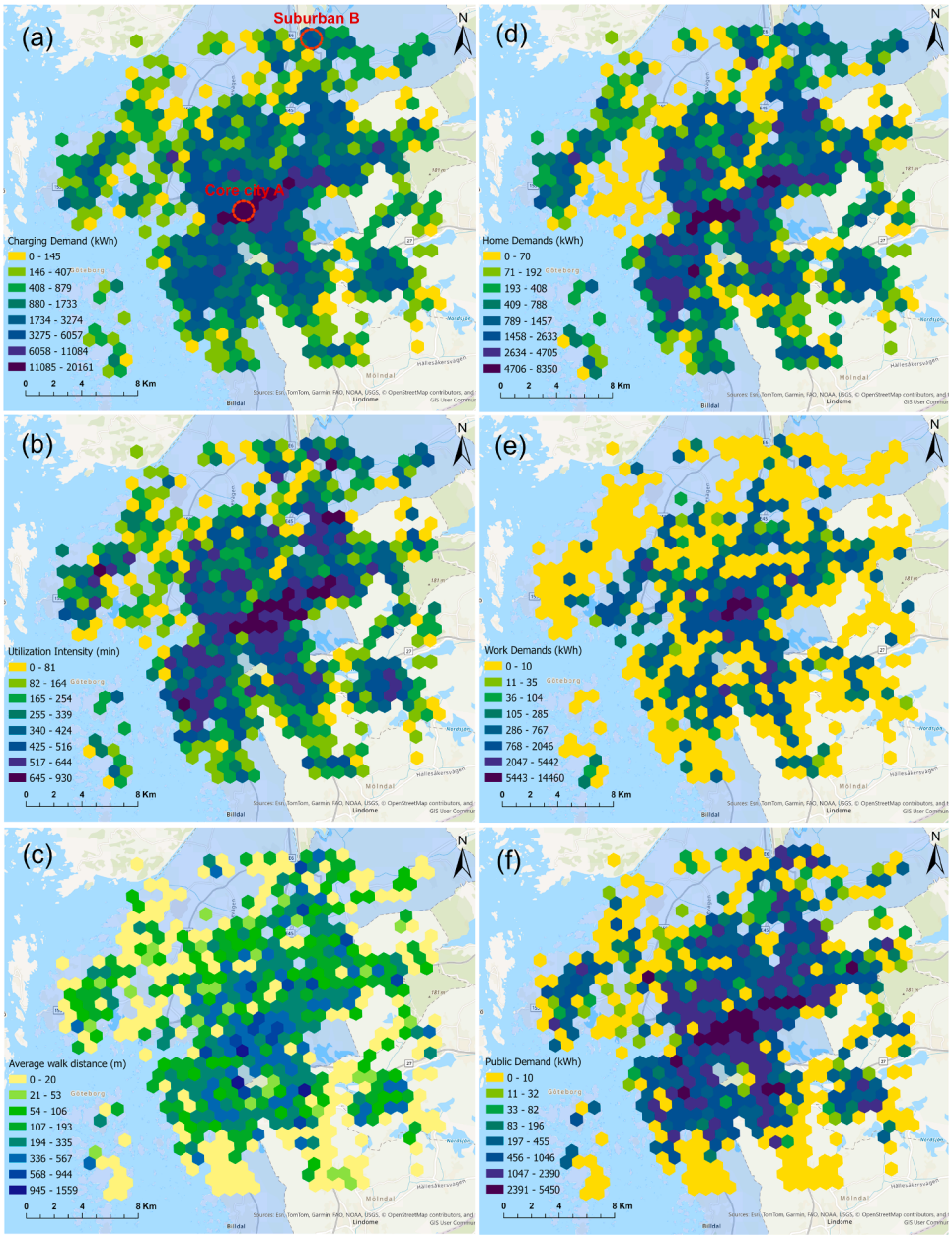

Fig. 6. Hexagon-aggregated metrics across Gothenburg Region A: (a) Total daily charging demand (kWh/day), (b) Mean charging duration per event (min), (c) Mean walking distance per event (m), (d) Home charging demand (kWh/day), (e) Work charging demand (kWh/day), (f) Public charging demand (kWh/day).

taining statistically robust demand and utilisation indicators. Across the region, total daily charging demand per hexagon (Fig. 6(a)) ranges from 6 kWh to 20 161 kWh, with a median of 871 kWh and a standard deviation of 778 kWh. The highest-demand cells in the historic core (Inom Vallgraven and central Göteborg) therefore deliver almost 20 MWh/day, whereas a large share of suburban hexagons in areas such as Askim, Torslanda, and Partille remain below 1 MWh/day. This confirms a pronounced spatial skew, with a small cluster of central cells concentrating a substantial fraction of system-wide energy throughput.

Home, work, and public charging exhibit similarly uneven spatial distributions. Home charging per hexagon reaches up to 8 344 kWh/day (median 418 kWh, standard deviation 362 kWh), concentrated in dense residential districts such as Majorna and Frölunda Torg (Fig. 6(d)). Workplace charging peaks at 14 456 kWh/day (median 251 kWh, standard deviation 710 kWh) along employment corridors including Lindholmen Science Park and Chalmers (Fig. 6(e)). Public charging attains 5 442 kWh/day (median 177 kWh, standard deviation 449 kWh) at major retail and transport hubs such as Nordstan, Heden, and Frölunda Torg (Fig. 6(f)).

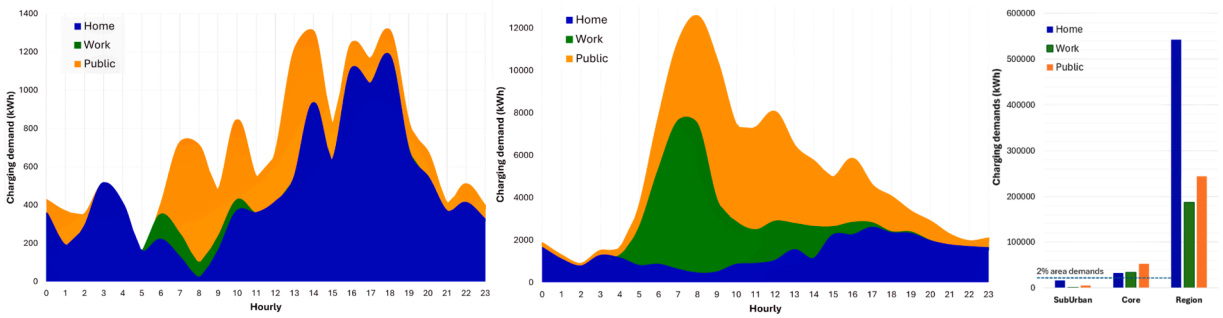

Fig. 7. Hourly charging demand by location type (a) in Surte (left) and (b) Central Gothenburg (center), and (c) daily totals by type (right).

These patterns are consistent with empirical analyses in western Sweden, which identify charger location and power rating as key determinants of spatial demand coincidence and local grid stress (Kazemtarghi et al., 2024; Hartvigsson et al., 2022).

Utilisation intensity, measured as mean charging-session duration, varies from less than 81 minutes in peripheral cells to approximately 645–930 minutes in central clusters around Lindholmen and Gamlestaden (Fig. 6(b)). Cells in the upper tail of total daily demand almost always fall into these long-duration classes, indicating that charging hotspots combine high energy throughput with plugs that are occupied for large fractions of the day. By contrast, fringe zones exhibit shorter, more opportunistic sessions. Mean walking distance to the nearest charger (Fig. 6(c)) ranges from 0–20 m in compact neighbourhoods with abundant on-site or home charging to 945–1 560 m in low-density islands such as the Öckerö archipelago and the outer southern suburbs. Walking distances substantially above 300 m approach or exceed typical comfort thresholds for everyday facilities (Daniels and Mulley, 2013), suggesting that spontaneous charging is likely to be suppressed in these areas.

To translate these hex-level diagnostics into actionable planning guidance, the hexagons are classified using simple quantitative thresholds. High-intensity demand hotspots are defined as cells with total daily demand above 10 000 kWh/day. These are confined to a small cluster in the mixed-use city core and, given their combination of very high energy throughput and long utilisation durations, are flagged as priority locations for adding clustered 11–22 kW AC capacity and, where grid constraints permit, additional 50 kW (or higher) DC fast chargers with active load management. Home-dominated hotspots are cells where home charging exceeds 4 700 kWh/day and accounts for more than 60 % of local energy use. In such districts, including Majorna and Frölunda Torg, further residential or neighbourhood AC chargers should be prioritised to accommodate evening and overnight loads. Workplace corridors are hexagons with work charging above 5 400 kWh/day and a work share exceeding 50 %, mainly around Lindholmen and Chalmers. Here, a mix of higher-power AC and selected DC chargers within employment centres is appropriate, together with load management to avoid daytime congestion. Public-access hubs are cells with public charging above 2 400 kWh/day and a public share exceeding 40 %, typically located at major retail and interchange nodes such as Nordstan, Heden, and Frölunda Torg. These are natural candidates for expanding public DC fast-charging capacity and improving queue management.

Finally, underserved residential areas are defined as hexagons with moderate total demand (above 1 000 kWh/day) but mean walking distance above 300 m. These peripheral locations, which include parts of the Öckerö archipelago and the outer southern suburbs, are highlighted as priorities for equity driven deployment of additional home-proximate AC chargers within roughly 200–300 m of residential clusters. Overall, the hexagon based diagnostics reveal strong spatial heterogeneity in both charging demand and access conditions and provide a direct mapping from simulated demand surfaces to corridor and neighbourhood scale siting recommendations for new or upgraded charging infrastructure.

5.4. Localized charging demand patterns

To illustrate the spatial variation in temporal charging demand of different zones, two hexagons were selected: a suburban cell in Surte (Ale municipality) and an urban core cell in Inom Vallgraven (central Gothenburg), as indicated in Fig. 6(a). Fig. 7(a), (b) shows their hourly charging profiles, while the right panel compares daily energy totals.

In the Surte suburban region, charging demand remains modest and temporally diffused over the 24-hour period (refer Fig. 7(a)). Home charging exhibits late-afternoon and early-evening maxima between 16:00 and 18:00, peaking at 1,174 kW at 18:00, driven by plan-ahead sessions to exploit off-peak ToU rates. Workplace charging remains negligible (maximum 132.5 kW at 06:00), and public charging peaks at 652 kW at 13:00, with a smaller shoulder of about 605 kW already visible at 08:00. Summed over 24 hours, Surte delivers about 11.1 MWh via home chargers, 0.5 MWh at workplaces, and 4.7 MWh at public stations (about 16.3 MWh in total), corresponding to roughly 1.7 % of the region's daily charging demand. In contrast, the central Gothenburg zone exhibits concentrated peaks reflecting dense mixed-use activity. Workplace charging surges to 7,034 kW at 07:00–08:00 hours, reflecting intense demand along office corridors in the Vallgraven region. Public charging peaks at 6,534 kW at 09:00 hours, and home charging peaks at 2,548 kW at 17:00 hours. Daily aggregates reach 32,256 kWh (home), 33,854 kWh (work), and 52,102 kWh (public), collectively accounting for about 12 % of regional demand while covering less than 3 % of the study area.

These localized profiles highlight the impact of land-use intensity and charger availability on shaping demand. In Surte, the dominance of home charging and low workplace use suggests that additional public or workplace chargers could enhance midday

flexibility. In central Gothenburg, the pronounced morning workplace peak and substantial public station use indicate a need for high-capacity fast chargers and dynamic load management at key nodes to prevent queuing and maintain service quality. Linking hexagon-level temporal profiles with spatial metrics thus enables targeted infrastructure deployment of neighborhood-scale chargers in suburban locales and high-power DC fast chargers in urban cores, to optimize both accessibility and utilization.

6. Conclusions

This research advances charging demand estimation by incorporating a cost-responsive and adaptive smart charging user behavior into the MATSim agent-based modeling framework, enabling accurate and insightful near-future predictions. Recognizing critical methodological gaps such as behavioral heterogeneity and sensitivity to charging costs, this research explicitly models the interactions between travel behaviors and charging decisions influenced by spatiotemporal electricity pricing and smart charging. Key findings are summarized as follows.

- Incorporating dynamic and ToU tariffs in charging demand estimation shifts most daytime charging from workplaces to homes and moves the system-wide peak from a morning, workplace-dominated spike to a residential evening peak. This highlights the need to explicitly account for tariff effects in the accurate estimation of spatiotemporal charging demand, and the deficiencies of the existing literature that have overlooked these aspects.
- Probabilistic smart charging behavior reshapes spatiotemporal charging demand significantly. Relative to the cost aware immediate-charging baseline, adaptive smart charging reduces the residential home peak from about 50 MW to 40 MW (a reduction of roughly 20 %) and increases the share of daily home-charging energy delivered in low-tariff night hours (22:00–06:00) from about 25 % to 36 %, without materially changing total daily demand.
- There is pronounced charging behavioral heterogeneity among agents with identical trip chains. Spatiotemporal charging costs and adaptive smart charging lead to divergent charging strategies among users to minimize their own overall costs. Such heterogeneity highlights the importance of incorporating price awareness and smart charging into the modeling of estimating spatiotemporal charging demand.
- There is significant variation in overall charging demand and the temporal charging demand profile across different areas of a city. This highlights the need for approaches such as agent-based modeling that consider both spatial and temporal factors affecting users' charging behavior. Central Gothenburg city zones, such as Inom Vallgraven, exceed 120 MWh/day across all charger types, whereas a representative suburban hexagon in Surte contributes around 16 MWh/day. Hourly charging demand profiles show workplace charging in the core peaking at 7 MW at 08:00 hours, whereas suburban demand is dominated by off-peak home charging with local hourly peaks of only about 1.2 MW.

In summary, this work offers a behaviorally rich and spatially explicit basis for evaluating demand-side measures and infrastructure strategies, featuring a behaviorally nuanced estimation of EV charging demand that links activity patterns, state of charge, and dynamic tariffs. It thus lays a groundwork for subsequent studies that aim to co-optimize charging infrastructure designs and pricing strategies, supporting the sustainable expansion of urban electromobility. Even though this research fills several gaps in the literature, there are some limitations that need to be addressed in future work. A key limitation is that public charging is modeled at the access charger with power, access type, and a charger level tariff, without station specific tariffs, plug competition, or queuing. The reported outputs should therefore be interpreted as unconstrained demand surfaces rather than station level throughput trajectories. Where station operations are of interest, the same behavioral cost formulation can be combined with MATSim configurations that explicitly represent plug capacities and waiting/queue dynamics, as demonstrated in recent MATSim neighborhood-scale EV infrastructure studies (Kreuschner and Schlenther, 2025). The present implementation further employs static, annually averaged ToU multipliers and behavioral parameters calibrated to stylized but empirically grounded targets for Gothenburg. Validation against local smart-meter or operator data remains a priority as real-time pricing structures, new charging technologies, and evolving travel patterns are likely to alter charging choices over time. Extending the framework to handle real-time prices, explicit grid-constraint feedback, and vehicle-to-grid interactions would deepen policy relevance, while empirical calibration of range anxiety and price awareness distributions, combined with multi-city transferability tests, would enhance robustness. All tariff and behavioral parameters are exposed at the configuration level, so the same integrated model can, in principle, be re-estimated for other study regions once suitable data become available. In relation, the present implementation represents anticipation of future charging needs via weekly plan scoring and replanning. Explicit optimization of SoC and expenditures over longer multi-day horizons, including rare high-energy trips, is left for future work. Moreover, the current analysis does not decompose the marginal contribution of intra-activity, adaptive smart charging deferral versus MATSim's co-evolutionary replanning. A clean counterfactual comparison between a *deferral only* configuration (with frozen strategy modules) and the full joint replanning setup is prioritized for future work. Another future direction would be a systematic sensitivity and uncertainty analysis around the key behavioral and infrastructure parameters, such as the awareness and coincidence factors, the SoC threshold, home charger penetration, and the ToU profile, to quantify how strongly different calibrations influence peak-shifting magnitudes and spatial hotspot patterns in other contexts. Finally, coupling the demand model developed here with optimization routines for charger siting, storage sizing, and power-system reinforcement can turn the simulated demand surfaces into implementable infrastructure and grid investment plans, enabling integrated transport and energy planning based on behaviorally rich charging demand forecasts (Parishwad et al., 2025a).

Role of the funding source

The funders had no role in the study design, collection, analysis, or interpretation of data, writing of the report, or the decision to submit the article for publication.

CRediT authorship contribution statement

Omkar Parishwad: Writing – review & editing, Writing – original draft, Visualization, Validation, Software, Methodology, Investigation, Formal analysis, Data curation; **Kun Gao:** Writing – review & editing, Writing – original draft, Validation, Supervision, Project administration, Methodology, Investigation, Funding acquisition, Formal analysis, Conceptualization; **Arsalan Najafi:** Writing – review & editing, Writing – original draft, Validation, Supervision, Methodology, Investigation, Formal analysis, Conceptualization.

Data availability

The data used in this study are available from the corresponding author on reasonable request. To support transparency and reproducibility, the simulation code and a sample dataset are available in the UrbanEV-v2 GitHub repository.

Declaration of competing interest

The authors declare that they have no known competing financial interests or personal relationships that could have appeared to influence the contents of this manuscript.

Acknowledgment

The research is funded by JPI Urban Europe and Energimyndigheten (e-MATS, P2023-00029) and supported by Area of Advance Transport at Chalmers University of Technology. Any opinions, findings, conclusions, or recommendations expressed in this paper are those of the authors and do not necessarily reflect the sponsors' views.

Appendix A. Spatial distribution of simulated chargers

The spatial distribution of simulated charging stations in Gothenburg, Sweden includes Home chargers (7kW), Work chargers (11 kW), and Public chargers (22 kW) as discussed in Section 4. This Fig. A.1 illustrates the geographic deployment of charger types across the regional network, as prescribed by the modeling framework.

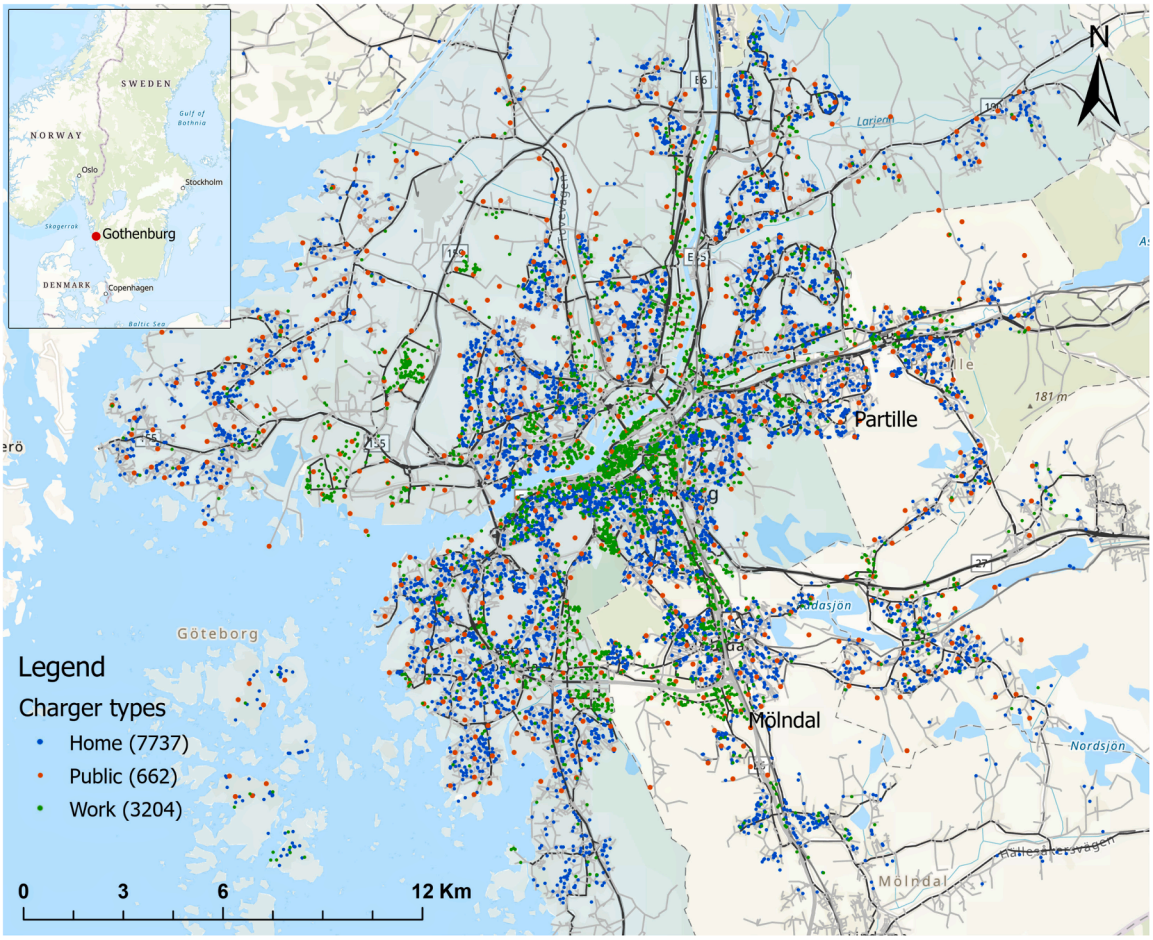

Fig. A.1. Spatial distribution of all the simulated chargers.

References

Adenaw, L., Lienkamp, M., 2021. Multi-criteria, co-evolutionary charging behavior: an agent-based simulation of urban electromobility. World Electric Veh. J. 12 (1), 18. https://doi.org/10.3390/wevj12010018

Arabani, H.P., Ingelström, M., Márquez-Fernández, F.J., Alaküla, M., 2024. Electric road systems for electric vehicle long-distance travel: a multi-agent simulation approach. In: 2024 IEEE International Conference on Electrical Systems for Aircraft, Railway, Ship Propulsion and Road Vehicles & International Transportation Electrification Conference (ESARS-ITEC). IEEE, Naples, Italy, pp. 1–6. https://doi.org/10.1109/ESARS-ITEC60450.2024.10819876

Bakhtiari, A., Patwary, A. U.Z., Ciari, F., 2023. Electric vehicle charging pricing design for agent-based traffic microsimulation. Procedia Comput. Sci. 220, 755–762. https://doi.org/10.1016/j.procs.2023.03.100

Bakhtiari, A., Zaman Patwary, A.U., Ciari, F., Moeini, A., Hajebrahimi, A., 2024. A comparative analysis of time-based and hybrid pricing models for electric vehicle charging. Procedia Comput. Sci. 238, 757–762. https://doi.org/10.1016/j.procs.2024.06.088

Berlin, T., Nagel, K., Kickhöfer, B., Horni, A., Zurich, E., Charypar, D., A Closer Look at Scoring, In Horni, A., Nagel, K., Berlin, T. (Eds.), in: ETH Zürich, The Multi-Agent Transport Simulation MATSim, (2016) pp. 23–34 Ubiquity Press. https://doi.org/10.5334/baw.3

Brulin, S., Toyooka, T., Fischer, L., Rodemann, T., Kreuchauff, F., 2025. Simulation of electric mobility concepts: swappable batteries and battery swapping stations. In: Proceedings of the 7th International Electric Vehicle Technology Conference (EVTeC 2025). Society of Automotive Engineers of Japan, Inc. (JSAE), Yokohama, Japan, pp. 1–6. Paper code 20259072. Preprint hosted by Honda Research Institute Europe.. https://www.honda-ri.de/pubs/pdf/6194.pdf.

Börjesson, M., Eliasson, J., 2014. Experiences from the Swedish value of time study. Transp. Res. Part A Policy Prac. 59, 144–158. https://doi.org/10.1016/j.tra.2013.10.022

Celik, O.S., 2024. Electric vehicle charging stations: model, algorithm, simulation, location, and capacity planning. Heliyon 10 (7), e29153. https://doi.org/10.1016/j.heliyon.2024.e29153

Daniels, R., Mulley, C., 2013. Explaining walking distance to public transport: the dominance of public transport supply. J. Transp. Land Use 6 (2), 5–20. https://doi.org/10.5198/jtlu.v6i2.308

Deb, S., Tammi, K., Kalita, K., Mahanta, P., 2018. Review of recent trends in charging infrastructure planning for electric vehicles. WIREs Energy Environ. 7 (6), e306. https://doi.org/10.1002/wene.306

Dharmakeerthi, C.H., Mithulananthan, N., Saha, T.K., 2014. Impact of electric vehicle fast charging on power system voltage stability. Int. J. Electric. Power Energy Syst. 57, 241–249. https://doi.org/10.1016/j.ijepes.2013.12.005

Ensslen, A., Ringler, P., Dörr, L., Jochem, P., Zimmermann, F., Fichtner, W., 2018. Incentivizing smart charging: modeling charging tariffs for electric vehicles in German and French electricity markets. Energy Res. Soc. Sci. 42, 112–126. https://doi.org/10.1016/j.erss.2018.02.013

ETH Zürich, Waraich, R.A., Bischoff, J., Berlin, T., Electric vehicles, In: ETH Zürich, Horni, A., Nagel, K., Berlin, T., (Eds.), The Multi-Agent Transport Simulation MATSim, Ubiquity Press (2016) 93–96, https://doi.org/10.5334/baw.14

Ge, Y., MacKenzie, D., 2022. Charging behavior modeling of battery electric vehicle drivers on long-distance trips. Transp. Res. Part D Transp. Environ. 113, 103490. https://doi.org/10.1016/j.trd.2022.103490
Göberndorfer, L., Savanovic, M., Jäger, G., 2024. Charging rush hour: modeling peak electricity demand for charging a fully electric fleet. Sage Open 14 (4), 21582440241290044. https://doi.org/10.1177/21582440241290044
Hartvigsson, E., Taljegard, M., Odenberger, M., Chen, P., 2022. A large-scale high-resolution geographic analysis of impacts of electric vehicle charging on low-voltage grids. Energy 261, 125180. https://doi.org/10.1016/j.energy.2022.125180
He, D., Yang, Y., Morichetta, A., Wu, J., 2025. Drone to recharge electric vehicles: operations, benefits, and challenges. Commun. Transp. Res. 5, 100162. https://doi.org/10.1016/j.commtr.2025.100162
He, S., Luo, S., Sun, K.K., 2022. Factors affecting electric vehicle adoption intention: the impact of objective, perceived, and prospective charger accessibility. J. Transp. Land Use 15 (1), 779–801. https://doi.org/10.5198/jtlu.2022.2113
Hörl, S., Ludwig, O., Rewald, H., Axer, S., 2025. Simulating individual charging behaviour in MATSim. In: Extended Abstracts of the MATSim User Meeting 2025 (MUM 2025). MATSim Association, Munich, Germany, pp. 1–3. Extended abstract submitted for presentation at MUM 2025.. https://matsim.org/conferences/mum2025/abstracts/MUM25_paper_19.pdf.
International Energy Agency, 2023. Global EV Outlook 2023: Catching up with Climate Ambitions Global EV Outlook. OECD. https://doi.org/10.1787/cbe724e8-en
Kamana-Williams, B., Bishop, D., Hooper, G., Chase, J.G., 2024. Driving change: electric vehicle charging behavior and peak loading. Renew. Sustain. Energy Rev. 189, 113953. Publisher: Elsevier BV. https://doi.org/10.1016/j.rser.2023.113953
Kazemtarghi, A., Mallik, A., Chen, Y., 2024. Dynamic pricing strategy for electric vehicle charging stations to distribute the congestion and maximize the revenue. Int. J. Electric. Power Energy Syst. 158, 109946. https://doi.org/10.1016/j.ijepes.2024.109946
Kim, Y., Kim, S., 2021. Forecasting charging demand of electric vehicles using time-series models. Energies 14 (5), 1487. https://doi.org/10.3390/en14051487
Kreuschner, M., Schlenther, T., 2025. Simulation of daily charging behaviour in MATSim: a case study of das neue gartenfeld in berlin. In: Extended Abstracts of the MATSim User Meeting 2025 (MUM 2025). MATSim Association, Munich, Germany, pp. 1–4. Extended abstract submitted for presentation at MUM 2025. https://matsim.org/conferences/mum2025/abstracts/MUM25_paper_28.pdf.
Kuehnel, N., Rewald, H., Axer, S., Zwick, F., Findeisen, R., 2022. Flow-inflated selective sampling: efficient agent-based dynamic ride-sharing simulations. Arbeitsberichte Verkehrs- und Raumplanung , 22Artwork Size: 22 p. Medium: application/pdf Publisher: ETH Zurich. https://doi.org/10.3929/ETHZ-B-000569127
Li, Z., Bian, Z., Chen, Z., Ozbay, K., Zhong, M., 2024. Synthesis of electric vehicle charging data: a real-world data-driven approach. Commun. Transp. Res. 4, 100128. https://doi.org/10.1016/j.commtr.2024.100128
Liao, Y., Tozluoglu, C., Sprei, F., Yeh, S., Dhamal, S., 2023. Open synthetic data on travel and charging demand of battery electric cars: an agent-based simulation on three charging behavior archetypes. https://doi.org/10.5281/ZENODO.7549847
Lin, B., Ghaddar, B., Nathwani, J., 2021. Electric vehicle routing with charging/discharging under time-variant electricity prices. Transp. Res. Part C Emerging Technol. 130, 103285. https://doi.org/10.1016/j.trc.2021.103285
Lin, W., Wei, H., Yang, L., Zhao, X., 2024. Technical review of electric vehicle charging distribution models with considering driver behaviors impacts. J. Traff. Transp. Eng. (English Edition) 11 (4), 643–666. https://doi.org/10.1016/j.jtte.2024.06.001
Liu, F., Shafique, M., Luo, X., 2024. Unveiling the determinants of battery electric vehicle performance: a systematic review and meta-analysis. Commun. Transp. Res. 4, 100148. https://doi.org/10.1016/j.commtr.2024.100148
Llorca, C., Moeckel, R., 2019. Effects of scaling down the population for agent-based traffic simulations. Procedia Comput. Sci. 151, 782–787. https://doi.org/10.1016/j.procs.2019.04.106
MATSim Community, 2025. MATSim electric vehicles (ev) contribution (contribs/ev). Maven artifact org.matsim.contrib:ev:2026.0-2025w38 https://mvnrepository.com/artifact/org.matsim.contrib/ev/2026.0-2025w38. repository by MATSim: https://repo.matsim.org/repository/matsim/
Menter, J., Fay, T.-A., Grahle, A., Göhlich, D., 2023. Long-distance electric truck traffic: analysis, modeling and designing a demand-oriented charging network for germany. World Electric Veh. J. 14 (8), 205. https://doi.org/10.3390/wevj14080205
Moeckel, R., Kuehnel, N., Llorca, C., Moreno, A.T., Rayaprolu, H., 2020. Agent-based simulation to improve policy sensitivity of trip-based models. J. Adv. Transp. 2020, 1–13. https://doi.org/10.1155/2020/1902162
Muratori, M., Alexander, M., Arent, D., Bazilian, M., Cazzola, P., Dede, E.M., Farrell, J., Gearhart, C., Greene, D., Jenn, A., Keyser, M., Lipman, T., Narumanchi, S., Pesaran, A., Sioshansi, R., Suomalainen, E., Tal, G., Walkowicz, K., Ward, J., 2021a. The rise of electric vehicles–2020 status and future expectations. Progress Energy 3 (2), 022002. https://doi.org/10.1088/2516-1083/abe0ad
Muratori, M., Jadun, P., Bush, B., Hoehne, C., Vimmerstedt, L., Yip, A., Gonder, J., Winkler, E., Gearhart, C., Arent, D., 2021b. Exploring the future energy-mobility nexus: the transportation energy & mobility pathway options (TEMPO) model. Transp. Res. Part D Transp. Environ. 98, 102967. https://doi.org/10.1016/j.trd.2021.102967
Nord Pool, 2024. Day-ahead prices (area prices), hourly, SE3. Accessed July 2024. https://data.nordpoolgroup.com/auction/day-ahead/prices.
Novosel, T., Perković, L., Ban, M., Keko, H., Pukšec, T., Krajačić, G., Duić, N., 2015. Agent based modelling and energy planning – utilization of MATSim for transport energy demand modelling. Energy 92, 466–475. https://doi.org/10.1016/j.energy.2015.05.091
Parishwad, O., Gao, K., Najafi, A., 2025a. Joint optimization of charging infrastructure and renewable energies with battery storage considering user redirection incentives. https://doi.org/10.2139/ssrn.5395539
Parishwad, O., Jia, R., 2023. Prospects of the activity-based modelling approach: a review of sweden's transport model- SAMPERS. In: Bie, Y., Gao, K., Howlett, R.J., Jain, L.C. (Eds.), Smart Transportation Systems 2023. Springer Nature Singapore, Singapore. Vol. 356, pp. 139–148. Series Title: Smart Innovation, Systems and Technologies. https://doi.org/10.1007/978-981-99-3284-9_13
Parishwad, O., Jiang, S., Gao, K., 2023. Investigating machine learning for simulating urban transport patterns: a comparison with traditional macro-models. Multimodal Transp. 2 (3), 100085. https://doi.org/10.1016/j.multra.2023.100085
Parishwad, O., Najafi, A., Liu, X., Gao, K., 2025b. The role of renewable energy to promote future electric transport and power systems. In: The Routledge Handbook of Sustainable Urban Transport. Routledge, London, 1st edition. pp. 361–373. https://doi.org/10.4324/9781003425489-30
Patil, P., Kazemzadeh, K., Bansal, P., 2023. Integration of charging behavior into infrastructure planning and management of electric vehicles: a systematic review and framework. Sustain. Cities Soc. 88, 104265. https://doi.org/10.1016/j.scs.2022.104265
Qiang, Y., Zhou, Y., Gebreyesus, G.D., Fujimura, S., 2025. Multi-agent trips simulation-based charging demand forecasting. IEEJ Trans. Electr. Electron. Eng. 20 (8), 1219–1228. https://doi.org/10.1002/tee.70022
Rietmann, N., Hügler, B., Lieven, T., 2020. Forecasting the trajectory of electric vehicle sales and the consequences for worldwide CO2 emissions. J. Clean Prod. 261, 121038. https://doi.org/10.1016/j.jclepro.2020.121038
Rodrigues, R., Pietzcker, R., Sitarz, J., Merfort, A., Hasse, R., Hoppe, J., Pehl, M., Ershad, A.M., Baumstark, L., Luderer, G., 2023. 2040 greenhouse gas reduction targets and energy transitions in line with the EU Green Deal. https://doi.org/10.21203/rs.3.rs-3192471/v1
Rostami, A., Verbas, O., Ghafarnezhad, B., Soltanpour, A., Ghamami, M., Zockaie, A., 2024. Exploring impacts of electricity tariff on charging infrastructure planning: an activity-based approach. Transp. Res. Part D Transp. Environ. 136, 104451. https://doi.org/10.1016/j.trd.2024.104451
Schüßler, M., Niels, T., Bogenberger, K., 2017. Model-based estimation of private charging demand at public charging stations. Eur. J. Transp. Infrastruct. Res. https://doi.org/10.18757/EJTIR.2017.17.1.3185
Sevdari, K., Calearo, L., Bakken, B.H., Andersen, P.B., Marinelli, M., 2023. Experimental validation of onboard electric vehicle chargers to improve the efficiency of smart charging operation. Sustain. Energy Technol. Assess. 60, 103512. https://doi.org/10.1016/j.seta.2023.103512
Shariatzadeh, M., Lopes, M. A.R., Henggeler Antunes, C., 2025. Electric vehicle users' charging behavior: a review of influential factors, methods and modeling approaches. Appl. Energy 396, 126167. https://doi.org/10.1016/j.apenergy.2025.126167
Shukla, M., Singh, D.K., Yadav, A., Singh, A.K., Jumaa, N.A., Mohammed, A., 2023. Optimizing electric vehicle charging station placement in urban areas: a data-driven approach. In: 2023 3rd International Conference on Advance Computing and Innovative Technologies in Engineering (ICACITE). IEEE, Greater Noida, India, pp. 2835–2838. https://doi.org/10.1109/ICACITE57410.2023.10183075

Sun, X.-H., Yamamoto, T., Morikawa, T., 2015. Charge timing choice behavior of battery electric vehicle users. Transp. Res. Part D Transp. Environ. 37, 97–107. https://doi.org/10.1016/j.trd.2015.04.007

Tan, J., Liu, F., Xie, N., Guo, W., Wu, W., 2022. Dynamic pricing strategy of charging station based on traffic assignment simulation. Sustainability 14 (21), 14476. https://doi.org/10.3390/su142114476

Thorhauge, M., Rich, J., Mabit, S.E., 2024. Charging behaviour and range anxiety in long-distance EV travel: an adaptive choice design study. Transportation https://doi.org/10.1007/s11116-024-10561-x

Tozluoglu, C., Dhamal, S., Yeh, S., Sprei, F., Liao, Y., Marathe, M., Barrett, C.L., Dubhashi, D., 2023. A synthetic population of Sweden: datasets of agents, households, and activity-travel patterns. Data Brief 48, 109209. https://doi.org/10.1016/j.dib.2023.109209

Visaria, A.A., Jensen, A.F., Thorhauge, M., Mabit, S.E., 2022. User preferences for EV charging, pricing schemes, and charging infrastructure. Transp. Res. Part A Policy Prac. 165, 120–143. https://doi.org/10.1016/j.tra.2022.08.013

Wang, J., Huang, C., He, D., Tu, R., 2023. Range anxiety among battery electric vehicle users: both distance and waiting time matter. Proc. Human Fact. Ergonom. Soc. Annu. Meet. 67 (1), 1309–1315. https://doi.org/10.1177/21695067231193669

Wongsunopparat, S., Cherian, P., 2023. Study of factors influencing consumers to adopt EVs (electric vehicles). Bus. Econ. Res. 13 (2), 155. https://doi.org/10.5296/ber.v13i2.21054

Wu, X., Yao, L., Yu, Y., Jiang, X., Wu, R., Gong, G., 2023a. Heterogeneous aggregation and control modeling for electric vehicles with random charging behaviors. IEEE Trans. Sustain. Energy 14 (1), 525–536. https://doi.org/10.1109/TSTE.2022.3219343

Wu, Y., Lu, Y., Zhu, Z., Holguín-Veras, J., 2023b. Optimizing electric vehicle charging infrastructure on highways: a multi-agent-based planning approach. Sustainability 15 (18), 13634. https://doi.org/10.3390/su151813634

Yi, Z., Chen, B., Liu, X.C., Wei, R., Chen, J., Chen, Z., 2023. An agent-based modeling approach for public charging demand estimation and charging station location optimization at urban scale. Comput. Environ. Urban Syst. 101, 101949. https://doi.org/10.1016/j.compenvurbsys.2023.101949

Zhan, W., Liao, Y., Deng, J., Wang, Z., Yeh, S., 2025. Large-scale empirical study of electric vehicle usage patterns and charging infrastructure needs. npj Sustain. Mob. Transp. 2 (1), 9. https://doi.org/10.1038/s44333-024-00023-3

Zhuge, C., Bithell, M., Shao, C., Li, X., Gao, J., 2021. An improvement in MATSim computing time for large-scale travel behaviour microsimulation. Transportation 48 (1), 193–214. https://doi.org/10.1007/s11116-019-10048-0

Zhuge, C., Shao, C., 2018. Agent-based modelling of locating public transport facilities for conventional and electric vehicles. Netw. Spatial Econom. 18 (4), 875–908. https://doi.org/10.1007/s11067-018-9412-3